Paper 4

Farzadi, P. & Alaei, B. (Submitted 2006). Stratigraphic architecture of the Zagros Basin: towards an objective comparison of the Fold-Thrust Belt and Foreland provinces. Submitted to the Journal of Petroleum Geology; under consideration for a thematic issue.

STRATIGRAPHIC ARCHITECTURE OF THE ZAGROS BASIN:

A COMPARISON OF THE FOLD-THRUST BELT AND FORELAND PROVINCES

P. Farzadi[1] and B. Alaei[2]

1 Department of Earth Science, University of Bergen, Allegt,41, N5007, Bergen, Norway,

Author for correspondence, email: Pourdad.Farzadi@geo.uib.no

2 Research Centre, Norsk Hydro, Oil & Energy, PO Box 7190, N5020, Bergen, Norway.

Abstract

The Zagros Basin is of the world's richest hydrocarbon provinces, but is still under-explored even after 90 years of production. As the most obvious accumulations have been located, many in structural traps, stratigraphic models are of increasing exploration importance. In this paper, we discuss models of regional and local stratigraphic evolution models which take account of Cretaceous and Tertiary deposition processes and deformation events. The paper is based on studies in hydrocarbon-producing regions which are in terms of their structural characteristics quite different: the Dezful embayment in the Zagros Fold and Thrust Belt and the SE Zagros Foreland Basin. Cretaceous reservoir facies in both areas were deposited before the formation of the fold-and-thrust belt. They are the result of depositional processes which were mainly controlled by eustatic sea-level variations, with second-order changes in relative sea level attributable to salt tectonism and regional deformation. Conventional seismic processing and analysis was not sufficient to resolve the stratigraphic relationships in both locations and to identify the reservoir facies necessary for this comparison, so this study also makes use of 3D prestack depth imaging and 3D multi-attribute analysis.

The regional stratigraphic trends presented here add sub-basin-scale details to models of Zagros Basin's evolution. Regional trends in stratal interval velocities provide a framework for evaluating trends in lithologic and porosity variation. Results show the Barremian quiescent deposition had a regionally-consistent southerly progradation, followed by the Aptian Dariyan Formation sub-basin development and consequent locally unique progradation directions as the Neo-Tethys rifted margins collapsed. Comparison of Kazhdumi Formation basal onlap patterns constrains the timing of Aptian salt mobilization and the distal effects of Neo-Tethys subduction, which was principally a foreland rather than a shelf-margin effect. Cenomanian stratigraphic trends delineate the shelf edge, together with various local basins now encompassed within the fold-and-thrust belt. The Turonian unconformity, which corresponds to initial Eurasia-Arabia continental collision, caused uplift and deep karstification in mid-platform locations (present-day foreland basin), but is scarcely recorded on the shelf edge. Post-Turonian tectonic activity resulted in the development of the previously-unrecognized carbonate turbidite systems which may have reservoir potential. A detailed comparison of these developments within the fold belt and within the Zagros foreland Basin will contribute to the understanding of both discovered oilfields and future plays.

Keywords: *Zagros Foreland Basin, Zagros Foldbelt, Persian Gulf, Principal Component Analysis, Prestack Depth Imaging.*

INTRODUCTION

This study compares the stratigraphic evolution of the Dezful Embayment in the highly-deformed Zagros Fold-and-Thrust belt with the relatively undeformed SE Zagros Foreland Basin. This comparison is based on subsurface stratigraphic and structural interpretations constrained by geophysical and well data from two onshore and two offshore oilfields. The four oilfields discussed (the *Karanj* and *Parsi*, and *Sirri C-D* fields: Fig. 1) are approximately 900 km apart. The Dezful Embayment is a prolific oil province (Patinson and Takin, 1972; Favre, 1975; Motiei, 1995; Sepehr, 2000; Sherkati and Leteuzey, 2004) which contains some 8% of global oil reserves (Bordenave and Hegre, 2005). In this study the *Karanj* and *Parsi* oilfields (Fig. 1) are used as examples of oil accumulation in structurally complex area. By contrast, the *Sirri* oilfields were chosen as representative of the fields in the Zagros Foreland Basin which has a far simpler tectonic history. Different methods of seismic data analysis were used in these two areas. Thus, investigation of the structurally-complex *Karanj* and *Parsi* fields require advanced seismic imaging techniques, whereas in the relatively undeformed *Sirri C-D* locations, multiple attribute analysis and interpretation was used to study the internal architecture of reservoir intervals. In both areas, high-density 3D seismic data, well logs, check shots, VSP, and core material were available.

These different approaches, used in areas of different structural complexity provided new information for the assessment of the subsurface geology.

The *Karanj* and *Parsi* oilfields, Zagros Foldbelt

In highly deformed terrains, it is necessary to rely on structural models for seismic interpretation of structure and stratigraphy, given that the quality of the seismic images will be poor (Bally, 1983; Mitra and Fisher, 1992; Alaei, 2005). Structural complexities include steeply dipping beds, overturned beds, complex thrust fault geometries, multiple detachment levels and thrust vergence, repeated intervals, and asymmetric folds associated with thrusts. In the Zagros Fold and Thrust Belt, these structural complexities are complicated by laterally variable stratigraphic thicknesses, as well as by an incompetent and internally-faulted and folded shallow cover which is deformed in a disharmonic style with respect to the underlying section (Favre, 1975; Mapstone, 1978). The lateral and vertical heterogeneities, especially in the velocity structure, make seismic imaging here a challenging task, resulting in poor target illumination (Alaei, 2006; Alaei and Pajchal, 2006).

The Karanj oil field (Fig. 1) in Dezful embayment was explored in 1963. Its main reservoir is the Asmari Formation with 650 m oil column and the production rate of 252000 barrels/day. The recoverable hydrocarbon is estimated as 1.65 billion barrels of oil and 3.5 TCF gas (Motiei, 1995). The Parsi oil field, north of the Karanj oil field was explored in 1964. Its main reservoir is the Asmari Formation with the production rate of 241000 barrels/day. The recoverable hydrocarbon is estimated as 3 billion barrels of oil and 9 TCF gas (Motiei, 1995).

Recognition of the subsurface complexity and the resolving limitations of processed seismic data are keys to selecting the best imaging method. Forward seismic modelling of geological structures can be used as a strategy for evaluating different imaging methods (Fagin, 1991). Prestack depth imaging can provide a more accurate subsurface image than some other methods (Yan and Lines, 2001). The technique does not follow the assumptions made in conventional data processing, which smear reflections from steeply-dipping beds. The velocity estimation is based on a structurally-consistent global tomographic method (Alaei, 2006). An integrated migration-velocity estimation approach (Alaei, 2006), based on both grid-based and horizon-based depth tomography, was applied to the *Karanj-Parsi* 3D dataset. Among advanced migration methods, the Kirchhoff migration (Schneider, 1978; Yan and Lines, 2001) is particularly popular; the quality of Kirchhoff prestack depth-migrated images improves considerably when constrained by hard geological information.

The *Sirri C-D* fields, Zagros Foreland Basin

The *Sirri* area in the SE Persian Gulf (Fig.1) is relatively undeformed, but stratal geometries are complex at the *Sirri C-D* oilfields. This complexity is attributed to deposition during a period of major sea-level change (Farzadi, 2005). The extensive Cretaceous carbonate platforms, which host important hydrocarbon accumulations in the NE Arabian Plate, are well documented (e.g. Murris, 1980; Harris and Frost, 1984; Jordan et al., 1985; Hughes Clark, 1988; Sharief et al., 1989). However the potential of the heterogeneous Cretaceous carbonate reservoirs offshore SE Iran is less well understood.

The *Sirri* D oil field was explored in 1971. The main reservoir is the Mishrif Formation (Sarvak in Zagros) with 300 million barrels of recoverable oil. The *Sirri* C oil field was explored two years later in 1973 with 185 million barrels of recoverable oil in the Mishrif Formation (Motiei, 1995).

A statistical technique known as Principal Component Analysis (Gurney, 1997) can be used to expand the interpretation content of 3D attribute volumes (Mari et al., 1999; Coléou et al., 2003; Linari et al., 2003). By reducing data noise and redundancy, Principal Component Analysis significantly increases the quality of the resulting 3D volumes for facies classification, and can help to visualize complex carbonate systems by increasing the seismic resolution. Extracted facies patterns are more diagnostic and easier to correlate than are conventional wiggle traces. This technique was applied to 3D seismic data from the *Sirri C* and *D* fields.

GEOLOGICAL SETTING

The Zagros area was part of the stable passive margin of Gondwanaland during most of the Palaeozoic, with deposition of shallow-water sediments including the Infra-Cambrian Hormoz salt (Glennie, 2000; Bahroudi and Koyi, 2004; Sepehr and Cosgrov, 2004). Later movement of the Hormoz salt played an important role in structural deformation, and the salt has also acted as a detachment horizon (Koop, 1977; Koop and Stonely, 1982; Beydoun et al., 1992; Sepehr and Cosgrove, 2004).

From the Late Permian to the Triassic, Arabian plate rifted from Central Iran with the opening of Neo-Tethys, with deep-water sedimentation along the rift and shallow-marine sedimentation along the marginal basins to the SW (Setudehnia, 1978; Koop and Stoneley, 1982; Beydoun et al., 1992; Sepehr and Cosgrove, 2004). The Tethys began to close with Early Cretaceous (Aptian?) subduction of oceanic crust beneath Central Iran (Glennie, 2000) (Fig. 2). The onset of compression had regional effects. A major relative sea-level fall, attributed to a compressional event in the Late Aptian (Fig. 2), is recognized as a regional unconformity throughout the Middle East (Harris et al., 1984; Sharland et al., 2001). Salt-diapirism corresponding with the Late Aptian compression is observed SE offshore Iran (Farzadi, 2005, 2006b). The Late Cretaceous (Santonian-Campanian?) closure of Neo-Tethys resulted in SW obduction of oceanic crust along the margin of the Arabian plate. Continued shortening resulted in intense faulting and thrusting along the Zagros Foldbelt, with renewed salt diapirism, the onset of folding in the Oman Mountains, and the formation of a regional highly karstified Turonian exposure surface (Loucks and Sarg, 1993; Pascoe et al., 1995; Montenat et al., 1999; Farzadi, 2006a). This compression continued until the central Iranian Plate and the Arabian Peninsula collided in the Maastrichtian (Glennie, 1995, 2000). Ocean-floor sediments were thrust onto the NE margin of the Arabian plate as a result of this collision.

The Late Cretaceous represents a period of major change in the area of the present-day Zagros Foreland Basin (Loutfi et al., 1987; Burchette, 1993; Pasco et al., 1995; Droste and Steenwinkel, 2004; Farzadi, 2005, 2006a). Regression at the end of the Cretaceous left most of the Arabian Plate emergent apart from local areas in the northern UAE and the Zagros Basin. Subsequent transgression in the Paleogene resulted in shallow-marine conditions over most of the Arabian Plate, although deep-water conditions prevailed in the Zagros and the Ras-Al-Khimah Basin (Oman), which were separated by the emergent Fars Arch (Kazerun line).

In the Paleocene to Early Eocene, the Zagros Basin became separated from Neo-Tethys for the first time. A rapid transgression in the Late Eocene marked a return to more open-marine conditions. Then, during the Late Eocene-Oligocene regression, the Zagros Basin, while not exposed, nearly disappeared as a distinctive depocenter, and this eustatic sea- level fall led to widespread emergence across the Arabian Plate. An early-mid Oligocene transgression is marked by open-marine facies close to the base of the Asmari Formation. The mid-Oligocene global sea-level fall again restricted marine deposition in the Zagros Basin; this period is characterized by sabkhas and thick wedges of a deltaic siliciclastics.

Rifting of the Afro-Arabian plate during the Oligocene initiated development of the Red Sea, and uplift of the Arabian Shield provided a source of coarse clastics for the Zagros Basin from the SE. A major Mid-Oligocene sea-level lowstand caused a reactivation of fluvial systems (Ahwaz Sandstone, Fig. 2) with a marked unconformity at the base. Shallow-marine carbonates (Asmari Formation) dominated the Zagros Basin during the Mid-Oligocene. Rising sea level during the Early Miocene is recorded by the disappearance of the deltas and their replacement by shallow-marine carbonate systems. Marginal areas starved of clastic supply developed as coastal sabkhas (Kalhur Member, Fig. 2). Compressional folding began during or soon after the deposition of the Oligo-Miocene Asmari Formation (Fig. 2). Interpretation of well and seismic data suggests that the evaporites of the Lower Miocene Gachsaran Formation were deposited mainly in subsiding lows, with thickness variations controlled by several factors including tectonics. During the Plio- Pleistocene, low-angle thrusting and associated folding generated the present-day structural configuration (Mapstone, 1978; Sepehr and Cosgrove, 2004). The contact between the Upper Asmari Limestone and the Lower Gachsaran Evaporites is diachronous, implying progradation of coastal sabkhas across shallow-marine carbonates as the basin filled, possibly related to the westward growth of the Zagros Foldbelt. The halite sequences in the Gachsaran Evaporites indicate isolation and almost complete evaporation of the basinal waters.

The stratigraphy shown in Fig.2 consists of potential reservoir rocks and source rocks. The potential reservoir rocks include the Fahliyan, Gadvan, Dariyan, Mishrif, Sarvak, Ilam and Asmari Formations and the potential source rocks include the Kazhdumi, Khatiyah and Ahmadi Formations.

METHODOLOGY

Seismic Depth imaging at the *Karanj and Parsi* oilfields: Velocity analysis and Migration

In structurally and stratigraphically complex cases such as the Zagros Foldbelt the estimation of interval velocity must be based on more accurate methods, which includes forward modelling of the travel times (the modelled travel times) fit to observed travel times. Reflection tomography methods (e.g. Biondi, 2004) have been used in this study to update the interval velocity function. We have applied a hybrid tomographic approach (Alaei, 2006) comprising both grid-based and horizon-based tomography. Irrespective of the method used to estimate velocity, it is rare that one model uniquely satisfies the observed data. In other words the velocity determination problem is non-unique or is an ill-posed inverse problem. (Treitel and Lines, 2001). To constrain the velocity estimation process we have used different *a priori* information including detailed seismic interpretation, regional structural style, and well-derived information, such as sonic logs, check shots, and zero-offset VSP data. The velocity analysis is more data-driven at the early stages and model-driven at the final stages.

The geometry of acquisition in the Zagros Foldbelt is constrained by the rough topography and, as such, is seldom regular. The sensitivity of migration methods to irregularities in data-point distribution makes Kirchhoff Prestack depth migration preferable despite its limitations. The Kirchhoff method is less sensitive than other methods to irregular spatial sampling of 3D Prestack data. We have applied single-arrival Kirchhoff Prestack depth migration using a spherical coordinate system (Alaei and Pajchel, 2006), which approximates the wavefront geometry. The PSDM was constrained with data from more than 90 wells. The resulting image quality from the complex faulted anticlines is remarkably good.

The geometry and velocity of near-surface deposits represents a major challenge to successful imaging in areas with rough topography, such as the *Karanj and Parsi* locations. In depth imaging, a small error in near-surface velocity can introduce large errors in ray-path and travel-time calculations for underlying events, and can significantly deteriorate the seismic image at depth (Gray et al., 2001). Adjustments can be made to the field data to correct for such errors, in effect by placing all the reflection arrival times on a single datum to account for local differences in elevation and weathering-related low velocity materials (Cox, 1999). We used field static data and applied the prestack depth migration from a floating datum (a smoothed version of the topography).

3D seismic classification at the *Sirri* fields: Multiple attribute volumes and Data reduction

A 3D seismic facies classification technique was used on a combination of 3D attribute volumes using Paradigm's Seisfacies software at the *Sirri* fields in the Zagros Foreland Basin (*Sirri C-D*, Fig. 1). In the multiple-volume classification, the inputs data comprise several seismic versions (seismic attributes) to expand information content. Seismic data and generated attributes contain a huge number of data samples, all highly redundant and noisy (Coléou et al., 2003). Using a large number of input attribute volumes dramatically increases data redundancy. Attempts to reduce the data by removing redundant attributes may cause loss of information not immediately apparent as valuable to the interpreter (Linari et al., 2003).

Principal component analysis (PCA) is a statistical technique used for data reduction that preserves essential features of the seismic character. For computational simplicity, PCA can handle multiple variables simultaneously to find the principal directions of linearly transformed components that represent the transformations (Gurney, 1997) of the multivariate data (Kendall, 1975). It allows the representation of large sets of data in a new vectorial space with a smaller dimension than the original. This powerful data-driven algorithm describes the relationships between multiple variables with coordinates in a vectorial space, which represent their contribution to the new components. The procedure treats all available data volumes globally to reproduce the complex relationships among the variables.

Once the correlation matrix of the input attributes is known, standard linear algebraic techniques (singular value decomposition, Mari et al., 1999) can decompose the data matrix into a summation of eigenvalues and eigenvectors. PCA examines the pattern space and finds the principal directions of variances in the multidimensional data by determining the distributions of eigenvectors. Eigenvector analysis can reveal patterns and their correlations in the distribution of events in 3D space. In practice, the computed directions of the principal components correspond to the largest eigenvalues labeled in order of decreasing data variability. The newly generated data volumes (PCA components) defined by the contribution of all input attributes can now be used for the classification of the original seismic data. In the classification process, the assumption is that two samples have the same facies class if they are characterized by similar values in all input seismic attribute volumes and, therefore, likely to correspond to a similar geologic environment. The classification results are displayed as a volume in 3D space that is considered to be of fundamental importance. It can provide new geological and seismic stratigraphic information that existed, but was not apparent in traditional seismic volume.

RESULTS

Velocity studies

Interval velocity variations for the different formations (Fig. 2) were considered in this study. In general, although variations are introduced by the major structural trends that divide the mountain belt, regional interval velocities increase from the foreland towards the thrust belt. The Zagros Foldbelt is dominated by carbonates, in which velocity variations are dependent on depositional environment rather than depth (Anselmetti and Eberli, 1993). Non-carbonate units showed some depth-dependency.

We summarize velocity variations from the Barremian Gadvan Formation to Plio-Quaternary Bakhtiyari Formation in Table 1. There is no strong regional velocity trend for the Dariyan Formation; rather, velocity is controlled by depositional environment and post-depositional factors. The few cases of velocities lower than 5000m/s probably represent anomalously large porosity.

The velocity gradient of the Kazhdumi Formation is characteristically positive. Negative velocity gradients can be attributed to over-pressured zones. The overlying Sarvak carbonates have interval velocities over 5500 m/s, making the Kazhdumi-Sarvak boundary an important regional velocity inversion.

The interval velocity of the Asmari Formation including Gachsaran member 1 increases from the foreland (4000m/s) towards the mountain front (5750 m/s). This is true for the carbonates, but where the facies changes from Asmari carbonates to Ahwaz sandstone the velocity decreases to as low as 3500 m/s. In the anhydrite and salt Kalhur member of the lower part of the Asmari Formation interval velocity for the anhydrite exceeds 5000 m/s while that of the salt beds is 4450m/s.

The overlying Gachsaran Formation (Members 2 to 6) shows a clear regional velocity increase from the foreland towards the mountain front. The velocity of salt beds (mainly member 4) is more or less constant (4450m/s). The Gachsaran Formation varies in thickness; thick zones with an anomalously low percentage salt have correspondingly low interval velocities. At higher percentage salt the interval velocity does not change with thickness.

Stratigraphic architecture of the Zagros Foldbelt and Foreland Basin

In this section we discuss the uppermost Barremian through Santonian interval in the two study areas and compare the Zagros Foreland Basin with the Zagros Foldbelt. We also discuss the Tertiary of the foldbelt, in which major production comes from strongly deformed intervals.

Late Barremian to Aptian

(i) Zagros Foreland Basin

The Barremian to Aptian Gadvan Formation (James and Wynd, 1965; Motiei, 1993; Sharland at al., 2001) has been penetrated by only one well, at *Sirri C* field and this only penetrated its uppermost part. The well recorded green pyritic and glauconitic shales with a high gamma-ray response overlying argillaceous and pebbly limestones. The shaly unit may correlates with the Hawar Shales of the UAE (Boichard et al., 1995) and Qatar (Sugden and Standring, 1975), and with the uppermost marls within the Kharaib Formation in Oman (Hughes Clarke, 1988; Simmons, 1994). The time-equivalent Biyadh Formation in Saudi Arabia includes thin beds of limestones within a green shale dominated succession (Shebel and Alsharhan, 1994). At the *Sirri* fields, limestones including Dictyoconnus arabicus are assigned to the Khalij Member of the Gadvan Formation (Motiei, 1993), and underlie the uppermost shaly unit.

Neither seismic nor well data alone provide a full picture of the subsurface architecture of the Gadvan Formation at *Sirri* oilfields. Seismic data indicates the variability at the top of the formation but not within it, because of the low impedance contrasts. Well and seismic data forms a complementary data set at the *Sirri* fields, and combination of the two data sets has improved the geologic model of the Gadvan Formation (Fig. 3a).

A second-order transgression in Hauterivian/ Barremian times (Sharland et al., 2001) culminated in a maximum flooding surface (K70 MFS of Sharland et al., 2001) within the shales at the top of the Gadvan Formation at the *Sirri* fields. The overall SE progradation of the uppermost Gadvan Formation (Fig. 3a) indicates that the Berriasian to Hauterivian third-order sea-level rise (Sharland et al., 2001) was buffered by an overall, second-order regression.

(ii) Zagros Foldbelt

In the *Karanj-Parsi* oilfields area, the Gadvan Formation comprises shales and argillaceous limestones with the Khalij carbonate member divides the Formation into upper and lower units. The Khalij carbonate system (Mid to Late Barremian) (Sharland et al., 2001) developed in the entire *Karanj-Parsi* oilfields (Fig. 4a). The Gadvan shales and carbonates prograded to the NW, and were deposited during a marine transgression over the carbonates of the Fahliyan Formation (Khosravi Said, 1982). The Upper Gadvan thickens to the west (Fig. 4a).

(iii) Discussion

The contrast between the NW progradation of the Gadvan Formation in the Dezful Embayment and the SE progradation of the Upper Gadvan Formation at the *Sirri* fields (Fig. 3a, 4a) indicates the presence of separate intrashelf basins. A relatively high progradation-to-aggradation ratio, in the absence of a landward facies shift, suggests that carbonate production outpaced the increase in accommodation space, which resulted from subsidence of the NE Arabian Plate (Koop and Stoneley, 1982; Sharland et al., 2001) associated with the onset of subduction in northern Tethys. The time-equivalent Zubair deltaic sandstones, which developed during the highstand in the north-central Arabian Plate (Sharland et al., 2001) are interpreted not to have reached the *Sirri C-D* or *Karanj-Parsi* areas.

The Late Aptian Transgression

The Early Cretaceous terminated with a widespread Aptian transgression which blanketed most of the earlier deposits (Koop and Stoneley, 1982; Hughes, 2000; Terken et al., 2001; Fisher et al., 1997; Immenhauser et al., 2001; Montenat et al., 2003). In the SE Zagros foreland Basin, the rudistid reefs assigned to the Shu'aiba Formation (equivalent to the Dariyan Formation) flanked local intrashelf clastic basins (e.g. Calavan et al., 1992). The Dariyan Formation was deposited in a regional shelf-to-basin complex, resulting in progradational mounds visible in seismic records (Farzadi, 2006b). A lowstand- or shelf-margin wedge of the equivalent Shu'aiba Formation (Bab Shale member) is present in the UAE (Aldabal and Alsharhan, 1989; Fischer et al., 1997), but is probably only thinly developed in the SE Zagros Foreland Basin. In the UAE, exploration and development wells indicate that the reservoir quality in the Shu'aiba Formation is closely related to primary depositional facies, with the best quality encountered in prograding carbonate build-ups (e.g. Calavan et al., 1992; Fisher et al., 1997; Borgomano et al., 2002; Droste and Steenwinkel, 2004; Farzadi, 2006b).

(i) Zagros Foreland Basin

In the *Sirri* area in the SE Zagros Foreland Basin, seismic facies classification shows a complex prograding pattern within the Dariyan Formation. The pattern indicates lateral variations in depositional facies and thus lithology within the Dariyan carbonate build-ups. The classification extended through an interval of 70 ms two-way-time (ca. 150m), making it possible to visualize the 3D pattern of the build-up's distribution. Seismic-scale build-ups (the red and yellow facies classes in Fig. 3b) characterize the middle part of the Dariyan Formation. The isochor map of the Dariyan Formation in Fig. 3f has a relatively constant thickness suggesting that tectonism and regional differential subsidence were not important during deposition, and that its complex internal patterns are the results of eustasy, siliciclastic influx and other environmental changes in the Zagros Foreland Basin area.

The basin-wide Aptian marine transgression was abruptly terminated by a major pre-Albian regression that resulted in development of an erosional surface marking the top of the Dariyan Formation (Koop and Stoneley, 1982) in the Zagros Foldbelt and the Shu'aiba Formation in the SE Zagros foreland Basin (Sharland et al., 2001).

(ii) Zagros Foldbelt

Transgression and sediment deposition was re-established in the latest Aptian to early Albian (Immenhauser et al., 1999; Hughes, 2000; Sharland et al., 2001). Marine transgression in the *Karanj-Parsi* area of the Zagros Foldbelt during the Albian resulted in deposition of the shales and limestones of the Kazhdumi Formation which filled the preceding basin topography. Fig. 4b shows a prestack depth-migrated seismic profile across the *Karanj-Parsi* area illustrating the onlap of lower Kazhdumi strata on the Aptian (top-Dariyan Formation) unconformity.

(iii) Comparison

The Kazhdumi Shales, deposited above the Aptian unconformity in both the *Karanj-Parsi* and *Sirri* areas, are the distal equivalent of the deltaic Burgan Sandstones present to the NE. At *Sirri* the lower Kazhdumi similarly onlaps the Aptian unconformity (Fig. 3c). The diachronous nature of the Aptian transgression is apparent, with the base of the Kazhdumi Formation becoming progressively younger towards the crests of the *Sirri C* and *D* structures (Fig. 3c) and the *Karanj-Parsi* structures (Fig. 4b). The Kazhdumi Formation of southern Iran (James and Wynd, 1965) is an equivalent of the Nahr Umr Formation of the UAE (Sharland et al., 2001). The Kazhdumi isochor (Fig. 3e) shows the effects of pre-Albian salt diapirism, manifested as two thin circular zones over the *Sirri* domes. This Late Aptian diapirism of infra-Cambiran salt is contemporaneous with, and may be distally related to, the onset of the subduction of oceanic crust within Neo-Tethys II (Glennie, 2000).

Middle Cretaceous (Albian-Turonian)

(i) Zagros Foreland Basin

At *Sirri*, Kazhdumi Formation is capped by Orbitolina-rich carbonates (Sharland et al., 2001; Farzadi, 2006a) of the Maudud Formation (James and Wynd, 1965).This Formation was deposited in response to another rise in relative sea level with a waning clastic sediment supply, and is equivalent to the lower part of the Sarvak Formation in the Zagros Foldbelt.

At *Sirri*, the Maudud Formation, has a constant thickness of 20m, and passes upwards into the marls and wackstones with abundant plankton of the Khatiyah Formation indicating a continued rise in relative sea level (Farzadi, 2006a). The isochor map of the Khatiyah interval indicates a gradual thickening towards the NW (Fig. 5c). During this relative sea level rise, a slight positive relief developed in the area between the *Sirri C* and *D* domes, allowing the initiation and development of a carbonate platform (Fig. 5 a and e, Farzadi, 2006a). Progradation of this platform was halted by a major flooding event corresponding with the top of the Khatiyah Formation. This flooding event passes upward into a second carbonate platform, the Mishrif Formation, which shows progradation over large distances, and which is characterized by bioclastic packstones and grainstones with rudist debris. A centrally-located bank with an elevated rim at the top of the upper Mishrif platform is interpreted as a late- build-up which developed prior to Turonian emergence. At the top of the Mishrif Formation is an unconformity which takes the form of a highly karstified surface (Farzadi, 2005, 2006a).

Using the conventional seismic analysis and well ties, we were able to divide the Khatiyah and Mishrif Formations into seismic sequences (Farzadi, 2005, 2006a). However, we were not able to map geobodies such as the platform margins, isolated build-ups and flooding deposits in a horizontal dimension. However, Fig. 5b illustrates a stratal slice (Zeng et al., 1998; Farzadi, 2005, 2006b) chosen from sequential slices calculated throughout the seismic classification volume which, enabled mapping of an isolated platform margin.

(ii) Zagros Foldbelt

In the *Karanj-Parsi* area, the Sarvak Formation comprises Late Albian – Early Turonian carbonates and the lower Sarvak consists mainly of basinal (Oligostegina) facies. The area is located in a narrow intrashelf basin with shelf margins towards the south and the north (T'Hart, 1970; Bolz, 1978). Fig. 6a illustrates the palaeogeographic reconstruction of the lower Sarvak Formation. Fig 4b illustrates a seismic profile oriented perpendicular to the lower Sarvak basin trend as well as the progradation of carbonates from the NE towards *Parsi* field and Fig. 6b is another seismic profile presenting the progradation of carbonates from the southwest towards *Karanj* field. Shallow-water limestones have prograded into a narrow NW/SE trending intrashelf basin. The lower Sarvak depocenter within the Dezful Embayment was linked to the geometry of this intrashelf basin. Towards the basin margins (north of *Parsi* and south of *Karanj*), increasing amounts of slope limestones with rudist debris are interbedded with the Oligostegina facies (Figs. 4b. and 6b). A NW-SE-oriented build-up geometry within the lower Sarvak Formation (Fig. 6c) probably indicates the proximity of the *Parsi* area to the slope margin.

During the Cenomanian a restricted intrashelf basin developed within the Dezful Embayment (Bolz, 1978). At the *Karanj-Parsi* fields, the middle Sarvak Formation consists mainly of Oligosteginid limestones together with intervals of rudist biostromes. Mixed shales and carbonates developed towards the NE and SW showing a facies transition from inner ramp to middle ramp. In the mid Cenomanian to early Turonian, the upper Sarvak Formation limestone represents a transition from shallow-water open-marine conditions in the south, to deeper slope/basin conditions (Oligosteginid argillaceous limestones) in the north (Bolz, 1978). The carbonates of the upper Sarvak became emergent and eroded during the middle Turonian, but given the position of the fields, the resultant unconformity is not extensively developed here. The channel-like feature at the uppermost part of the Sarvak Formation shown in Fig. 6d, however, may be attributed to Turonian erosion (Fig. 2). The channel is at the *Parsi* field, which is close to the Kuh-e-Bangestan anticline where the Turonian unconformity is well developed. The Sarvak Formation in the *Karanj-Parsi* fields thickens from WNW to ESE indicating the NNE-SSW trend of uplift developed during the Late Turonian compression.

The Sarvak Formation carbonate build-up geometries are similar in the Zagros Foldbelt (Fig. 6c) and the Zagros Foreland. This indicates the importance of the Sarvak Formation for the development of stratigraphic traps.

Turonian-Palaeocene

(i) Zagros Foreland

The highly karstified Turonian unconformity surface at the *Sirri* fields is shown in plan view in Fig. 7d, based on integrated seismic classification. The Turonian unconformity is observed by the deep-water Laffan marls which pass upwards into the neritic/pelagic limestones of the Santonian Ilam Formation. This relative sea level rise is attributable to eustasy and perhaps compression-driven downward plate flexure.

In the *Sirri* area, a turbidite system developed within the deep-marine carbonates of the Ilam Formation (Fig. 7e). Analysis of the classification volume over stratal slices led to an interpretation of successive, north and south channel systems. Both channel systems and their terminal lobes were detected within the seismic classification cube. The facies associated within one of the channel branches has been cored, and consists of packstones and pebbly limestones with lithic components, encased in pelagic mud-rich carbonates. The only well that encountered an abandoned channel of the turbidite (well E1 in Fig.7) showed non-commercial oil within the Ilam Formation known as a non-reservoir unit.

(ii) Zagros Foldbelt

The regional transgression started late in the Turonian and effected the *Karanj-Parsi* area from the NE (e.g. Wells, 1968). This transgression carried argillaceous material of the Surgah Formation from the Zagros Foldbelt to the margins of the Arabian Shield. There was similar transgression-related erosion and transport in the SE Zagros, resulting in deposition of the Laffan Formation. As marine conditions spread onto the Arabian Shield, Surgah and Laffan marls progressively gave way laterally and in time to carbonates of the Ilam Formation (Wells, 1968). Fig. 8a shows interval velocities within the Ilam Formation in the *Karanj-Parsi* oilfield areas. Unit 1 is composed of about 10 m of shales (probably Surgah Formation) which can be correlated to the Laffan Shales in the SE Zagros foreland basin. Following the deposition of these shales, Ilam Formation deep-water limestones were deposited (units 2 and 4, Fig. 8a). A low velocity shale unit within the Ilam Formation (unit 3 Fig. 8a) was also deposited.

Following a minor but regional regression in the middle Campanian (Wells, 1968; T'Hart, 1970) which halted carbonate deposition, marine domination restarted in the late Campanian and the marls of the Gurpi Formation were deposited. In the *Karanj-Parsi* the Gurpi Formation onlaps the pre-existing NNE-SSW trending high. Fig. 8b shows interval velocity section from the Ilam, Laffan and part of the Sarvak Formations in the *Sirri C-D* fields. The difference in velocity between the carbonate units of the Ilam and Sarvak Formations is similar to that in the foldbelt. Fig. 8c illustrates the westward onlap of the Gurpi Formation on the Ilam Formation. At present, no detailed information on the uppermost Gurpi and Pabdeh Formations in the *Sirri* area is available.

Oligocene-Miocene

The Asmari Formation (Late Oligocene – Early Miocene) (James and Wynd, 1965) shows considerable lithofacies variations in *the Karanj-Parsi* oilfields. Asmari limestones were deposited within a mixed siliciclastic-carbonate ramp setting. The exposed Arabian Shield in SW Khuzestan provided material for the development of Oligocene and Early Miocene Ahwaz delta systems (Motiei, 1993). Ahwaz sandstones ranges in age from Oligocene to lower Miocene (James and Wynd, 1965), and thin bedded Ahwaz Sandstones are present at the *Karanj* field. The Sandstone beds dominate the lower part of the Asmari Formation. Fig. 9a is a PSDM seismic profile trending NE-SW which illustrates seismic response of the Ahwaz Sandstone Member within the lower part of the Asmari Formation at the *Karanj* oilfield. The lateral extension of the corresponding reflection event representing the contact between the sandstone and carbonates indicates the limited extent of this member. Fig. 9b illustrates an interval velocity log within a Lower Miocene Ahwaz sandstone interval. In the *Parsi* field, the Miocene (James and Wynd, 1965) Kalhur Member evaporite was deposited to the NW (Fig. 10a). The thickness of this member varies from more than 140m in the NW to zero in the centre of the field. The halite layer thins from the NW towards the centre of the field where it pinches out, overlain by a basal anhydrite layer. The reflection characteristics of halite are distinct from those of anhydrite. Discontinuous, patchy reflection events are characteristic of halite beds in the NW part of the profile (Fig. 10a). Fig. 10b illustrates the clinoforms of the Asmari Formation carbonates, indicating development of ramp margin towards the NE of the studied area.

Late Miocene, *Karanj-Parsi* oilfields

In the *Karanj-Parsi* fields, the thickness of the Gachsaran Formation (Late Miocene, James and Wynd, 1965) varies significantly. The upper part of the formation is partially exposed in the studied area. Well data and seismic interpretation results reveal the more or less uniform thickness of the uppermost part (Member 7) of the formation (Fig. 11). The main thickness variations took place in Members 4-2. Oswald (1978) attributed Gachsaran Formation thickness variations in the *Gachsaran* oilfield to four factors:

- changes in bedding attitude;

- decreases resulting from normal faulting;

- increase caused by thrust faulting, and parasitic folding; and

- Depositional thickness changes.

Oswald (1978) did not include thickness variation associated with syn-depositional salt flow or squeezing as suggested by Sherkati et al. (2005). Oswald (1978) did infer onlap geometries in the lower part of the Gachsaran Formation, and Sherkati et al. (2005) observed the same feature in the Dezful Embayment. Verges (2006 pers. Comm.) suggested that faulting was the main reason for thickness increases more or less as Oswald (1978) proposed. Our seismic stratigraphic observations in the *Karanj-Parsi* area within the lower part of the Gachsaran Formation (Fig.11) are consistent with an onlap geometry although in some cases it is difficult to distinguish between faulting and these stratigraphic features. Further seismic sedimentological studies are needed to make this clear.

Discussion

We used separate seismic approaches in two tectonically different provinces of the Zagros area to compare the interplay of Cretaceous and Tertiary depositional processes and deformation events responsible for reservoir development. The depositional processes were largely controlled by eustatic sea level variations, with by local, relative sea-level changes attributable to salt and regional tectonics. The main deformation events occurred in the Aptian, Turonian, Santonian/Coniacian and Late Miocene-Pliocene. In the *Karanj-Parsi* oilfields area, reservoir-critical depositional processes are largely obscured by the fold-thrust deformational overprint. Here, the seismic solution was careful PSDM validated by structural studies. The *Sirri* area lies in the foreland basin, and deformation events are more subtle. Here the reservoir-critical stratigraphic relations were resolved through multi-attribute seismic analysis guided by local and regional stratigraphic considerations. By comparing the fold-thrust belt and foreland study areas, we show that both areas contain a stratigraphy that is related to the other. The differences, sometimes subtle, place constraints on regional basin evolution. Examples are discussed below.

The Mid to Late Barremian Khalij carbonate system (Sharland et al., 2001) developed regionally and is identifiable at the *Karanj-Parsi* fields in the northern Dezful Embayment and the

Sirri C-D fields in the SE foreland basin. The progradation direction of the Barremian Gadvan Formation is different in these areas. NW progradation at the *Karanj-Parsi* fields contrasts with the SE progradation at *Sirri* and indicates the development of independent intrashelf basins. The NW thickening of the upper Gadvan Formation at *Karanj-Parsi*, in contrast to the constant thickness observed at *Sirri*, is interpreted to indicate NW-tilting and a higher rate of subsidence in the area of the present-day Zagros Foldbelt. Development of the Zubair deltaic sandstones NW of the Foreland Basin (Sharland et al., 2001; Motiei, 1993, 1995) is attributed to this subsidence. These sandstones, however, did not reach the *Karanj-Parsi* oilfields.

The direction of Gadvan Formation progradation in both study areas suggests that a NW-SE-elongated subsidence area developed perpendicular to the spreading trend of the Neo-Tethys. Identification of prograding clinoforms is essential to understanding the vertical and lateral distribution of potential stratigraphic traps. An example lies in the relation and transition to the laterally equivalent Kharaib Formation, which is one of the major oil-producing reservoirs in offshore Abu Dhabi (Saotome et al., 2000).

Continued subsidence from the Barremian to the Aptian resulted in a similar progradation direction associated with rudist build-up development within the Dariyan Formation. At *Sirri*, however, the thickness of the formation remains constant indicating little influence of extensional deformation in this area. In the *Karanj-Parsi* fields, the Dariyan Formation is seismically thinner (40 m) and deeper than at *Sirri* (110 m) resulting in less information and possibly leading to interpretive bias. Kazhdumi strata onlapping the Dariyan Formation in both study areas, and thinning of the Kazhdumi Formation over the crests of the *Sirri* structures, indicate local salt diapirism and a regional foreland-basin tectonic event possibly related to subduction. The absence of growth strata patterns within the Kazhdumi Formation indicates that this tectonic event occurred before Kazhdumi deposition. Investigation and comparison of other foldbelt and foreland basin subsurface data would help to resolve this issue, as well as other issues such as the amount of Dariyan Formation eroded at the Aptian unconformity.

The narrow NW-SE-trending lower Sarvak Formation basin with marginal mixed-facies (basin/platform or Oligostegina/rudist debris) is well documented in the *Karanj-Parsi* area (e.g.

T'Hart, 1970). The NW-SE-trending build-up at the northern flank of *Parsi* also confirms the basin trend, as well as the proximity of the *Parsi* field to the shelf. These relations are indicated by the PSDM data. The rapid facies changes at the *Karanj-Parsi* oilfields should be examined in detail as part of any future petroleum evaluation of the Sarvak Formation. The Oligosteginid argillaceous limestones of the intrashelf basin are present through the entire Upper Sarvak, indicating that deep-water conditions existed up to the Early Turonian.

Transgressive-regressive cycles in the Cenomanian Khatiyah and Mishrif Formation (Ahmadi and Sarvak in Zagros) created isolated and vertically-stacked platform-to-intrashelf topographies which have been documented in *Sirri* (Farzadi, 2006a). Isolated build-ups within these two formations are important for the development of low-risk stratigraphic traps (Farzadi, 2006). The transgressive, platform-initiating part of each cycle probably correlates with a major regional flooding event. A few million years of emergence (Scott, 1990) related to the initial phase of the collision between Eurasia and the Arabian margin (O'Conner and Patton, 1986; Warburton et al., 1990) formed a faulted, karstified surface at the top of the Mishrif Formation (Alsharhan and Narin, 1988; Alsharhan and Kendall, 1991; Pasco et al., 1995; Philip et al., 1995; Montenat et al., 1999; Sharland et al., 2001). The distribution of karst collapse features, for example, is of great importance since these dissolution features have direct impact on reservoir quality (Farzadi, 2006a). Conventional seismic interpretation, however, is not adequate for the task; further multi-attribute analysis is required.

It is probable that the deeper-water setting of the Turonian unconformity in the *Karanj-Parsi* area prevents its clear imaging. The channel-like feature observed in the uppermost part of the Sarvak Formation in the *Parsi* field close to the Kuh-e-Bangestan (where the Mid Cretaceous unconformity is well developed) could be an indication of Turonian tectonic activity.

In the SE Zagros foreland basin, the Ilam Formation is not considered to be a reservoir unit (Motiei, 1993, 1995). However, the Ilam Formation turbidite channel system reported in this study indicates a potential for stratigraphic traps. The Late Turonian regional transgression started with the deposition of Surgah shales in the *Karanj-Parsi* oilfields area followed by the deposition of the Ilam Formation carbonates. The mid-Campanian regression in the *Karanj-Parsi* area is represented by the Gurpi Formation onlapping on to the Ilam carbonates.

In the *Karanj-Parsi* fields, the Asmari Formation (Late Oligocene – Early Miocene) includes members with distinctly different lithofacies: siliciclastics; carbonates; and evaporites. The Kalhur evaporite member developed in the NW part of the *Parsi* field. Although the lower Asmari strata are present in the SE of the *Parsi* field, they appear to be missing in the NW, where the Kalhur member is developed. James and Wynd (1965) dated the Kalhur Member as Early Miocene, equivalent to the Middle Asmari Formation. Therefore, in the NW *Parsi* field, the Pabdeh Formation underlies the middle Asmari Formation, while the lower Asmari Formation exits in SE Parsi and the entire *Karanj* field. The Ahwaz sandstone member, locally developed in Karanj, represents the incursion of a sand-prone deltaic system.

The lowest member of the Gachsaran Formation developed with almost no thickness change in the *Karanj-Parsi* area. Structurally it is in contact with the Asmari Formation and is folded in a similar way. The thickness variations in Members 2 and 3 of the Gachsaran Formation reflect possible depositional thickness changes. An alternative interpretation, proposed by Verges (Personal communication) envisages fault-related thickness changes for these members (2 and 3). Member 4 is the thickest salt unit in the Gachsaran Formation. We interpret internal faulting and folding to be the primary contribution to thickness variation in this member rather than bulk salt flow. Internal deformation is also responsible for thickness variation of Members 5 and 6. The uppermost member of the Gachsaran Formation shows almost no thickness variation in the *Karanj-Parsi* area, as has been confirmed by interpretation of PSDM seismic data as well as more than 90 wells.

Conclusions

The structural complexity of the Zagros Foldbelt and the complex stratigraphic and velocity heterogeneities characteristic of build-ups in the Zagros Foreland basin present significant seismic imaging challenges. The lack of sufficiently high-resolution seismic imaging techniques has precluded the definition of reliable exploration models at both regional and field scales. In our study, we have used advanced imaging techniques to reveal the relations between major tectonic events and depositional processes in two distinct but related tectonic provinces within the northeastern Arabian plate.

The tectonostratigraphy of the Zagros Foreland and Zagros Foldbelt provinces are of fundamental importance in delineating regional reservoir models. The Aptian major tectonic event attributed to Neo-Tethys subduction affected both areas but with different intensities. We conclude that this tectonic event was more intense in the Zagros Foreland compared to the Zagros Foldbelt. This interpretation is supported by the regional distribution of the base Kazhdumi Formation onlaps associated with the Hormoz salt movement in the *Sirri* and localized distribution of these onlaps in the *Karanj-Parsi* oilfields.

Detailed stratigraphic interpretation of the Turonian Paleokarst and a prospect carbonate turbidite system within the overlying Ilam Formation in *Sirri* indicate that both the Turonian uplift and the Santonian-Coniacian downward were more intense than previously recognized. The more significant development of the Aptian and Turonian unconformities in the Zagros Foreland area compared to the foldbelt, suggests that compressional events in southeastern foreland basin started earlier than in the foldbelt.

The advanced geologically-constrained, prestack depth imaging we have used in examining the Zagros Foldbelt and the multi-attribute interpretation techniques applied in the SE Zagros Foreland Basin have each revealed geological detail not achieved by conventional seismic analysis. These detailed geological insights made it possible to correlate important aspects of the stratigraphic and tectonic history essential to future prospect evaluation.

Acknowledgements

The Authors are grateful to IOOC and NIOC for providing seismic and well data; Norsk Hydro, for technical and financial support; and the University of Bergen for its supportive administration. Special thanks to W. Wheeler, D. Hunt, I. Sharp, J. Pajchel, J. Verges for their valuable input, and K. Atakan for supervision. Journal review by C.G.H. Tiratsoo and informal review by K. Dixon are acknowledged with thanks.

Reference:

ALAEI, B., 2005. Seismic forward modeling of two fault-related folds from the Dezful embayment of the Iranian Zagros Mountains. Journal of Seismic Exploration, **14/1**, 13-30.

ALAEI, B., 2006. An integrated procedure for migration velocity analysis in complex structures of thrust belts. Journal of Applied Geophysics, **59**, 89-105.

ALAEI, B., and PAJCHEL, J., 2006. Single Arrival Kirchhoff Prestack Depth Migration of complex faulted folds from the Zagros Mountains, Iran. CSEG Recorder, **31/1**, 41-48.

ALSHARHAN, A.S., 1985. Depositional environment reservoir units evolution and hydrocarbon habitat of Shu´aiba Formation, Lower Cretaceous, Abu Dhabi, UAE. AAPG Bull, **69**, 899-912.

ALSHARHAN, A.S., 1989. Petroleum Geology of the United Arab Emirates. Journ. Petrol. Geol., **12**, 253-288.

ALSHARHAN, A.S., and KENDALL, C.G.St.C., 1991. Cretaceous chronostratigraphy, unconformities and eustatic sea-level changes in the sediments of Abu Dhabi U.A.E. Cretaceous Research, **12**, 379–401.

ALSHARHAN, A.S., and NARIN, A.E.M., 1988. A review of the Cretaceous formations in the Arabian Peninsula and Gulf, Part II. Mid Cretaceous (Wasia Group) stratigraphy and paleogeography. Journal of Petroleum Geology, **11**, 89–112.

ANSELMETTI, F., and EBERLI, G.P., 1993. Controls on sonic velocity in carbonates. Pure and Applied Geophysics, **141**, 287–323.

BAHROUDI, A., and KOYI, H.A., 2004. Tectono-sedimentary framework of the Gachsaran Formation in the Zagros foreland basin. Marine and Petroleum Geology, **21**, 1295-1310.

BALLY, A.W., 1983. Seismic expression of structural styles. Vol. 3 - Tectonics of Compressional provinces/strike slip tectonics. AAPG Studies in Geology Series, No. 15.

BIONDI, B., 2004. 3D seismic imaging. Stanford Exploration Project, 356.

BEYDOUN, Z.R., HUGHES CLARK, M.W., and STONELY, R., 1992. Petroleum in the Zagros Basin: A Late Tertiary Foreland Basin Overprinted onto the Outer Edge of a Vast Hydrocarbon-Rich Palaeozoic-Mesozoic Passive Margin Shelf. In: MACQUEEN, R. and LECKIE, D. (Eds), Foreland Basins and Foldbelts. AAPG, Mem. **55**, 309-339.

BOICHARD, R.A.P., AL-SUWAIDI, A.S., and KARAKHANIAN, H., 1995. Sequence Boundary types and related Porosity Evolutions: Example of the Upper Thamama Group in Field “A” Offshore Abu Dhabi, United Arab Emirates. In: AL-HUSSEINI, M.I., (Ed), Middle East Petroleum Geosciences, GEO'94. Gulf PetroLink, Bahrain, **1**, 191-201.

BOLZ, H., 1978. The palaeogeographical evolution during the Cretaceous in the Operating Area with special emphasis on the Bangestan Group. Oil Service Company (OSCO) Internal Report 1274.

BORDENAVE, M.L., and HEGRE, J.A., 2005. The influence of tectonics on the entrapment of oil in the Dezful Embayment, Zagros Foldbelt, Iran. Journ. Petrol. Geol., **28/4**, 339-368.

BORGOMANO J., MASSE, J.P. and ALMASKIRY, S., 2002. The lower Aptian Shu´aiba carbonate outcrops in Jebel Kkhdar, northern Oman: Impact on static modeling for Shu´aiba petroleum reservoirs. AAPG Bull. **86/9**, 1513-1529.

BURCHETTE, T.P., 1993. Mishrif Formation (Cenomanian–Turonian), southern Arabian Gulf: Carbonate platform growth along a cratonic basin margin. In: SIMO, J.A.T., SCOTT, R.W. and MASSE, J.P. (Eds) Cretaceous carbonate platforms. AAPG, Mem, **56**, 185–199.

CALAVAN, C.W., HAGERTY, R.M., MITCHELL, J.C., and SCHUTTER, S.R., 1992. Integrated reservoir study and modeling of the Shu´aiba Reservoir, Bu Hasa Field, Abu Dhabi, United Arab Emirates. ADNOC/SPE Proceedings, SPE 24509, 299-312.

COLÉOU T., POUPON, M. and AZBEL, K., 2003. Unsupervised seismic facies classification: A review and comparison of techniques and implementation. Interpreter's corner, The Leading Edge, October 2003, 942-953.

COX, M., 1999. Static corrections for seismic reflection survey. Society of Exploration Geophysicists.

DROSTE, H., and VAN STEENWINKEL, M., 2004. Stratal geometries and patterns of platform Carbonates: The Cretaceous of Oman. In: Seismic imaging of carbonate reservoirs and systems. AAPG Memoir, **81**, 185-206.

FAGIN, S. W., 1991. Seismic Modelling of Geologic Structures, Applications to Exploration Problems, Geophysical Development series, no.**2**, Society of Exploration Geophysicists.

FARZADI, P., 2005. Stratal geometries of the Cretaceous carbonate systems- Application of multiple volume attribute analysis to 3D seismic data from the Persian Gulf. Middle East to Far East Carbonate Reservoirs: Exploration, Development and Exploitation, Petroleum Exploration Society of Great Britain, Carbonate Conference, London, 15^{th} and 16^{th} November 2005.

FARZADI, P., 2006_a. The development of Middle Cretaceous carbonate platforms, Persian Gulf, Iran: Constraints from seismic stratigraphy, well and biostratigraphy. Petroleum Geoscience, **12**, 59-68.

FARZADI, P., 2006$_b$. Seismic facies analysis based on 3D multi-attribute volume classification, Dariyan Formation, SE Persian Gulf. Journ. Petrol. Geol. **29/2**, 1-16

FAVRE, G, 1975. Structures in the Zagros Orogenic Belt. Oil Service Company of Iran (OSCO) Internal report, number 1233.

FISCHER, K.C., MOELLER, U., and MARSCHALL, R., 1997. Development of an exploration concept for the Shu´aiba Formation (Thamama Group) using seismic sequence and facies analysis in combination with forward modeling. In: I. Palaz and K.J. Marfurt (Eds.), Carbonate Seismology. Geophysical Developments Series 6, Society of Exploration Geophysicists, 407-416.

GRAY, S. H., 2000. Interpretive seismic imaging in structurally complex areas. In Depth imaging of Foothills seismic data. Canadian Society of Exploration Geophysicists, 106-107.

GRAY, H. S., AND J. ETGEN, J. DELLINGER, and D. WHITMORE, 2001. Seismic migration problems and solutions. Geophysics, **66**, 1622-1640.

GLENNIE, K.W., 1995. The geology of the Oman Mountains: an outline of their origin. Scientific Press, Beaconsfield, UK.

GLENNIE, K.W., 2000. Cretaceous tectonic evolution of Arabia's eastern plate margin: A tale of two oceans. In: Alsharhan, A.S. and R.W. Scott, (Eds.) Middle East models of Jurassic/Cretaceous carbonate systems. SEPM, Spec. publ., **69**, 9-20.

GURNEY, K., 1997. An introduction to Neural network. UCL Press, 234p.

HARRIS, P.M., and FROST, S.H., 1984. Middle Cretaceous carbonate reservoirs, Fahud field and northwestern Oman: AAPG Bulletin, **68**, 649-658.

HARRIS, P.M., FROST, S.H., SEIGLIE, G.A. and SCHENEIDERMANN, N., 1984. Regional unconformities and depositional cycles, Cretaceous of the Arabian Peninsula. In: J.S. Schlee (Ed.), Interregional unconformities and hydrocarbon accumulation. AAPG Memoir, **36**, 67-80.

HUGHES CLARKE, M.W., 1988. Stratigraphy and Rock Unit Nomenclature in the Oil-Producing Area of Interior Oman. Journ. Petrol. Geol., **11**, 5-60.

HUGHES, G.W., 2000. Bioecostratigraphy of the Shu´aiba Formation, Shaybah field, Saudi Arabia. GeoArabia, **5** (4), 545-578.

IMMENHAUSER, A., SCHLAGER, W., BURNS, S.J., SCOTT, R.W., GEEL, T., LEHMANN, J., VANDERGAAST, S., and BOLDER-SCHRIJVER, L.J.A., 1999. Late Aptian to late Albian sea level fluctuations constrained by geochemical and biological evidence (Nahr Umr Formation, Oman): Journ. Of Sedimentary Research, **69/2**, 434-446.

IMMENHAUSER, A., VAN DER KOOIJ, B., VAN VLIET, A., SCHLAGER, W., and SCOTT, R.W., 2001. An ocean-facing Aptian-Albian carbonate margin, Oman. Sedimentology, **48**, 1187-1207.

JAMES, G.A. and WYND, J.G., 1965. Stratigraphic Nomenclature of the Iranian Oil Consortium Agreement Area. AAPG Bull, **49**, 2182-2245.

JORDAN, C.F., CONNALLY, T.C. and VEST, H.A., 1985. Middle Cretaceous carbonates of the Mishrif Formation, Fateh field, offshore Dubai. In: Roehl, P.O. & Choquette, P.W. (Eds) Carbonate petroleum reservoirs. Springer-Verlag, New York, 425-442.

KHOSRAVI SAID, A., 1982. Cretaceous sediments in SW Iran. National Iranian Oil Company (NIOC), Internal report number, 1301.

KENDALL, M., 1975. Multivariate analysis. London, Charles Griffin.

KOOP, W. J., 1977. The paleostructural history of SW Iran and its effect on hydrocarbon generation and entrapment. Oil Service Company of Iran (OSCO), internal report number 1292.

KOOP, W. J., and STONELEY, R., 1982. Subsidence History of the Middle East Zagros Basin, Permian to recent. In: KENT, P., BOTT, M.H.P., McKENZIE and WILLIAMS, C.A., (Eds), The evolution of Sedimentary Basins, Philosophical Transactions of the Royal Society of London, Part A, **305**, 149–168.

LINARI, V., SANTIAGO, M., PASTORE, C., AZBEL, K. and POUPON, M., 2003. Seismic facies analysis based on 3D multi-attribute volume classification, La Palma field, Maracaibo, Venezuela. *The Leading Edge*, January 2003, 32-36.

LOUCKS, R.G. and SARG, J.F., 1993. Carbonate sequence stratigraphy, recent development and applications. AAPG, Mem., **57**, 3–41.

LOUTFI, G., BASLAIB, S.M. and ABU HAMD, M. 1987. Cenomanian stratigraphic traps in western Abu Dhabi, U.A.E. Paper SPE 15684, presented at the 5th Middle East Oil Show, Bahrain, Society of Petroleum Engineers, 1–8.

MAPSTONE, N. B., 1978. Structural geology of structures of Dezful (north) Embayment. Oil Service Company of Iran (OSCO), internal report, Technical note **13/1978**.

MARI, J.L., GLANGEAUD, F., and COPPENS, F., 1999. Signal processing for geologists and geophysicists. Institut francais du pétrole, 458 PP.

MITRA, S. and FISHER, G.W., 1992. Structural Geology of Fold and Thrust Belts. The John Hopkins University Press, Baltimore, 254 pp.

MONTENAT, C., SOUDET, H.-J., BARRIER, P. and CHEREAU, A., 1999. Karstification and tectonic evolution of the Jabal Madar (Adam Foothills, Arabian Platform) during the Upper Cretaceous. Bulletin Centre Recherche Elf Exploration Production., **22**, 161–183.

MONTENAT, C., BARRIER, P., and SOUDET, H.J., 2003. Aptian faulting in the Haushi-Huqf (Oman) and the tectonic evolution of the southeast Arabian Platform-margin. GeoArabia, **8/4**, 643-662.

MOTIEI, H., 1993. Geology of Iran: Stratigraphy of Zagros. Geological Survey of Iran (in Farsi).

MOTIEI, H, 1995. Petroleum geology of Zagros-1. Geological Survey of Iran (in Farsi), 589pp.

MURRIS, R.J., 1980. Middle East: Stratigraphic evolution and Oil habitat. AAPG Bulletin, **64**, 597–618.

O'CONNER, S.J. and PATTON, T.L., 1986. Middle Cretaceous carbonate reservoirs, Fahud field and northwestern Oman, Discussion. AAPG Bulletin, **70**, 1799–1801.

OSWALD, D. H., 1978. The Gachsaran formation of Gachsaran field. Oil Service Company of Iran (OSCO), Internal report No. 1281.

PASCOE, R.P., EVANS, N.P. and HARLAND, T.L., 1995. The generation of unconformities within the Mishrif and Laffan formations of Dubai and adjacent areas: applications to exploration and production. In: Husseini, M.I. (ed.) Middle East Petroleum Geosciences, Geo' 94, **2**. Gulf PetroLink, Bahrain, 749–760.

PATTINSON, R., and TAKIN M., 1971. Geological significant of Dezful Embayment Boundaries. IOOC report No. 1166 (unpublished).

PHILIP, J., BORGOMANO, J. and AL-MASKIRY, S., 1995. Cenomanian–Early Turonian carbonate platform of northern Oman: Stratigraphy and Palaeoenvironments. Palaeogeography, Palaeoclimatology, Palaeoceology, **119**, 77–92.

SAOTOME, J.I., SHIBASAAKI, T., SHIKAMA, T. and KAWAGUCHI, k.I., 2000. Geological controls on pore geometry of upper Kharaib reservoir, Offshore Abu Dhabi, U.A.E. In: Alsharhan, A.S. and R.W. Scott, (Eds) Middle East models of Jurassic/Cretaceous carbonate systems. SEPM, Spec. publ., **69**, 287-297.

SCOTT, R.W., 1990. Chronostratigraphy of the Cretaceous carbonate shelf southeastern Arabia. In: Robertson, A.H.F., Searle, M.P. and Ries, A.C. (Eds) *The Geology and Tectonics of the Oman Region.* Geological Society, London, Special Publications, **49**, 89–108.

SCHNEIDER, W., 1978. Integral formulation for migration in two and three dimensions. Geophysics, **43**, 49-76.

SEPEHR, M., 2000. The tectonic significance of Kazerun Fault zone, Zagros fold-thrust belt, Iran. Ph.D. thesis, Imperial College of London.

SEPEHR, M., and COSGROV, J. W., 2004. Structural framework of the Zagros Fold-Thrust belt, Iran. Marine and Petroleum geology, **21**, 829-843.

SETUDEHNIA, A., 1978. The Mesozoic sequence in southwest Iran and adjacent area. Journ.Petrol. Geol., **1**(**1**), 3–42.

SHARIEF, F.A., MAGARA, K. and ABDULLA, H.M., 1989. Depositional System and Reservoir Potential of the Middle Cretaceous Wasia Formation in Central-Eastern Arabia. Marine and Petroleum Geology, **6**, 303-315.

SHEBEL, H.T., and ALSHARHAN, A.S., 1994. Sedimentary facies and hydrocarbon potential of Berriasian-Hauterician carbonates in Central Arabia, In: SIMMONS, M.D., (Ed.), Micropalaeontology and Hydrocarbon Exploration in the Middle East: London, Chapman & Hall, 159-174.

SHERKATI, S., and LETOUZEY, J., 2004. Variation of structural style and basin evolution in the central Zagros (Izeh zone and Dezful Embayment), Iran. Marine and Petroleum Geology, **21**, 535-554.

SHERKATI, S., MOLINARO, M., FRIZON DE LAMOTTE, D., and LETOUZEY, J., 2005. Detachment folding in the Central and Eastern Zagros fold-belt (Iran): salt mobility, multiple detachments and late basement control. Journal of Structural Geology, **27**, 1680-1696.

SHARLAND P. R., ARCHER R., CASEY S.M., DAVIS R.B., HALL S.H., HEWARD A.P., HORBURY A.D., and SIMMONS M.D., 2001. Arabian plate sequence stratigraphy. GeoArabia, Spec. Publ., **2**, 261-278.

SIMMONS, M.D., 1994. Micropalaeontological biozonation of the Kahmah Group (Early Cretaceous), Central Oman Mountains, In: SIMMONS, M.D.,(Ed), Micropalaeontology and hydrocarbon exploration in the Middle East: British Micropalaeontological Society Publication Series: London, Chapman & Hall, 177-220.

SUGDEN, W., and STANDRING, J.J., 1975. Qatar Peninsula. Lexique stratigraphique Internationale, III, 10b3.

T'HART, B.B., 1970. Upper Cretaceous Palaeogeography, Structural history and prospects of Khuzestan Province Iran. Iranian Oil Operating Companies (IOOC), Geological and Exploration division, Internal Report No. 1172.

TERKEN, J.M.J., FREWIN, N.L., and INDRELID, S.L., 2001. Petroleum systems of Oman: Charge timing and risks. AAPG Bull. **85/10**, 1817-1845.

TREITEL, S., and LINES, L. 2001. Past, present, and future of geophysical inversion-A new millennium analysis. Geophysics, **66**, 21-24.

WARBURTON, J., BURNHILL, T.J., GRAHAM, R.H., and ISSAC, K.P., 1990. The evolution of the Oman Mountains foreland basin. In: Robertson, A.H.F., Searle, M.P. & Ries, A.C. (Eds) The Geology and Tectonics of the Oman Region. Geological Society, London, Spec. Publ., **49**, 419–427.

WELLS, A. J., 1968. Lithofacies and geological history of post Sarvak upper Cretaceous sediments in southwestern Iran. Iranian Oil Operating Companies (IOOC), Geological and Exploration division, Internal Report No. 1120.

YAN, L., and LINES L., 2001. Seismic imaging and velocity analysis for an Alberta foothills seismic survey. Geophysics, **66**, 721-732.

ZENG, H., HENRY, S.C. and RIOLA, J.P., 1998. Stratal slicing: Part II. Real seismic data: Geophysics, **63/2**, 514-522.

Figure Captions

Fig. 1. Regional map (a) showing location of the Karanj-Parsi and *Sirri* C-D oil fields (red stars) studied here. The Karanj-Parsi lies within the Zagros Fold and Thrust Belt in an area called the Dezful Embayment. The *Sirri* study area lies in the southeastern Zagros Foreland basin. These two areas have been chosen to compare and better understand the regional factors controlling the stratigraphic architecture. A depth structure map on top of the Ilam Formation in Karanj and Parsi oil fields (b) and a time structure map on top of the Dariyan Formation in Sirri C and D oil fields (c) show the position of these structures.

Fig. 2. Stratigraphy and major tectonic events mentioned in the manuscript. Most of these correlate well between Zagros Fold Thrust Belt (ZFTB) and SE Zagros Foreland.

Table 1. Regional interval velocity variations from the Barremian Gadvan Formation to the Plio-Quaternary Aghajari and Bakhtiyari Formations.

Fig. 3. Profiles, maps and horizontal slices through the *Sirri* oil field dataset. (a), (b) and (c) are profiles through the seismic classification volume showing significant internal geologic features within the Gadvan, Dariyan and Kazhdumi Formations. (d) Shows a proportional slice calculated through the volume, conformable with the tops of the Dariyan and Gadvan Formations (see profile b). This illustrates the lateral distribution of rudist build-ups (light brown) developed within the middle Dariyan Formation. (e) Shows an isochor of the Kazhdumi Formation over the crests of the *Sirri* C and D domal structures indicating thinning over the domes, consistent with local doming resulting from salt diapirism after the deposition of the Dariyan Formation. (f) Isochor of the Dariyan Formation showing the near-constant thicknesses which indicates the doming post-dated it. Three gamma-ray-derived sequences (bottom) at well C1 are interpreted as sea level fluctuations, which generated the internal configuration observed within the Gadvan and Dariyan Formations. The top of sequence 3 is an unconformity overlain by Kazhdumi Onlapping strata (profile c), indicating sea level rise.

Fig. 4. Profiles from Prestack Depth Migrated (PSDM) 3D seismic reflection data. a) Interpreted PSDM section along the strike of the Karanj structure showing top Khalij carbonate system (Mid to late Barremian), upper Gadvan NW progradation, and top Dariyan (upper picked reflector).

The thickness of upper Gadvan increases towards NW. b) Interpreted PSDM profile normal to the strike of Parsi structure. The dotted horizon shows the top Kazhdumi-base Sarvak. Lower Kazhdumi strata onlap the Aptian unconformity, over this the lower Sarvak strata prograde SW, which confirms the existence of lower Sarvak intrashelf basin around Karanj-Parsi.

Fig. 5. Mid-Cretaceous seismic stratigraphy in *Sirri*: Seismic analysis of the classification volume and well ties allows the division of the Khatiyah and Mishrif Formations into seismic sequences. Developments of two vertically stacked carbonate platforms (1 and 2 in a) are shown. A proportional slice through the volume within the Mishrif/ Khatiyah interval (b) illustrates the lateral distribution of the upper platform margin (2 in a). (c) Shows the isochor evidence of a gradual thickness change within the Khatiyah Formation associated with tilting of the basin is shown. This NW tilting caused locally faster sea level rise. To the NW, carbonates drowned; to the southeast the platform growth kept pace only in shoal areas. A centrally located bank (3 in a) with an elevated rim at the top of the upper platform near well D1 is interpreted as a late-growth build-up developed prior to the Turonian emergence (Farzadi, 2006_a). The isochor showing the upper platform is shown in D. Two prograding platform complexes, consisting of laterally stacked clinoform wedges, are shown in relation to accommodation cycles interpreted from well logs (e).

Fig. 6. a) Paleogeographic reconstruction of the lower Sarvak Formation (modified from T'Hart 1970). The mixed shelf-intrashelf facies is expected NE of Parsi (Fig. 4b) and SW of Karanj (Fig. 6b). b) Interpreted PSDM section (SW-NE) from the Karanj structure shows the NE progradation of the lower Sarvak. The SW progradation of the lower Sarvak in Parsi (Fig. 4b) and NE progradation in Karanj (b) is consistent with the palaeogeographic reconstruction made by T'Hart (1970) (6a). c) NW-SE trending build-up at the northern flank of Parsi structure confirming the proximity of this structure to the shelf. d) Subtle channel-like feature near the top of Sarvak formation at the NE flank of Parsi may indicate Turonian unconformity.

Fig. 7. Wells C1 and E1 with their gamma-ray-derived accommodation cycles are shown tied to classification data (a, b and c). D: Map based on isochor, showing a Paleokarst system developed over the Turonian erosional surface (top Mishrif reservoir). Well C1 penetrated a karst collapse (sink hole, c). The production rate of this well (from K) is significantly greater than other wells. Mapping

these dissolution features (d) is necessary for future field development. (e) Map within the Santonian Ilam Formation showing a carbonate turbidite with two channeling systems. Channels turn counter clockwise rotation prior to terminal lobe formation. Offshore development of a turbidite within the pelagic Ilam Formation in *Sirri* is attributed to plate flexure during the Turonian major compressional event (Glennie, 2000). Isochor map of the Ilam Formation (e inset) indicates little differentiation in thickness of this formation during the deposition. Well E1, which penetrated an abandoned channel of the turbidite in map e, is the only well in *Sirri* producing (non commercial) oil from the non-reservoir Ilam Formation (interval T' in well E1).

Fig. 8. (a): Interval velocities in the Ilam and upper Sarvak Formations in Karanj-Parsi area from well logs. The Ilam Formation is here informally subdivided into four units. Unit 1 is about 10 m. of shales (probably Surgah Formation) that can be correlated to the Laffan shales in the southeastern Zagros foreland basin. Units 2 and 4 are deep water limestones of the Ilam Formation, whereas unit 3 is a low velocity. (b), Interval velocities in the Ilam, Laffan, and upper Sarvak (Mishrif) Formations in *Sirri* C-D from well logs. Note the Ilam carbonate velocities in both *Sirri* and Karanj-Parsi are at least 500 m/s lower than in the uppermost Sarvak carbonates. (c) NW-SE section along the strike of Parsi structure shows northwestward onlapping of the Gurpi Formation on the Ilam Formation. This onlapping is not visible on the SW-NE sections.

Fig. 9. NE-SW PSDM seismic section from the Karanj field, showing uppermost Cretaceous through Miocene strata. The Ahwaz sandstone member in the lower part of the Asmari Formation directly overlies the Pabdeh Formation. The lateral extension of this contact reflection event is limited, indicating the limited, local extent of the Ahwaz Member. b) Interval velocity log of the Asmari Formation from a well located on the seismic section shows the low velocity Ahwaz sand unit at the base of the Asmari Formation.

Fig. 10. a) SE-NW PSDM seismic section along the strike of the Parsi structure illustrating the seismic reflection characteristics of the Kalhur evaporite member, lower Asmari Formation. The white double arrows show the Asmari interval and the green double arrows show the Kalhur member. The seismic reflectivity character of halite is distinct from that of anhydrite. The discontinuous patches of reflection events (NW part of the section) are characteristic of halite beds; these die out towards SE

(close to the smaller green arrow). This interpretation is calibrated with more than 3 wells along the section. b) SW-NE detailed section showing reflections interpreted as clinoforms in the upper Asmari Formation carbonates. The SW-vergent clinoform geometry indicates the ramp margin developed to the northeast of the Dezful area.

Fig. 11 NW-SE PSDM section along the strike of the *Karanj* structure, showing thinning in the Gachsaran Formation (double arrows). The lower Gachsaran Formation mainly Members 2 and 3, appear to pinch out to the NW, indicated by dotted lines with arrows. We provisionally call this geometry "tectonic onlap", discussed in the text. Other authors have variously attributed Gachsaran thickness variation to deposition or deformation. The continuous, strong reflection at the top of the double arrows is the top of Member 6; above this, parallel reflections indicate the relatively-constant thickness of Member 7.

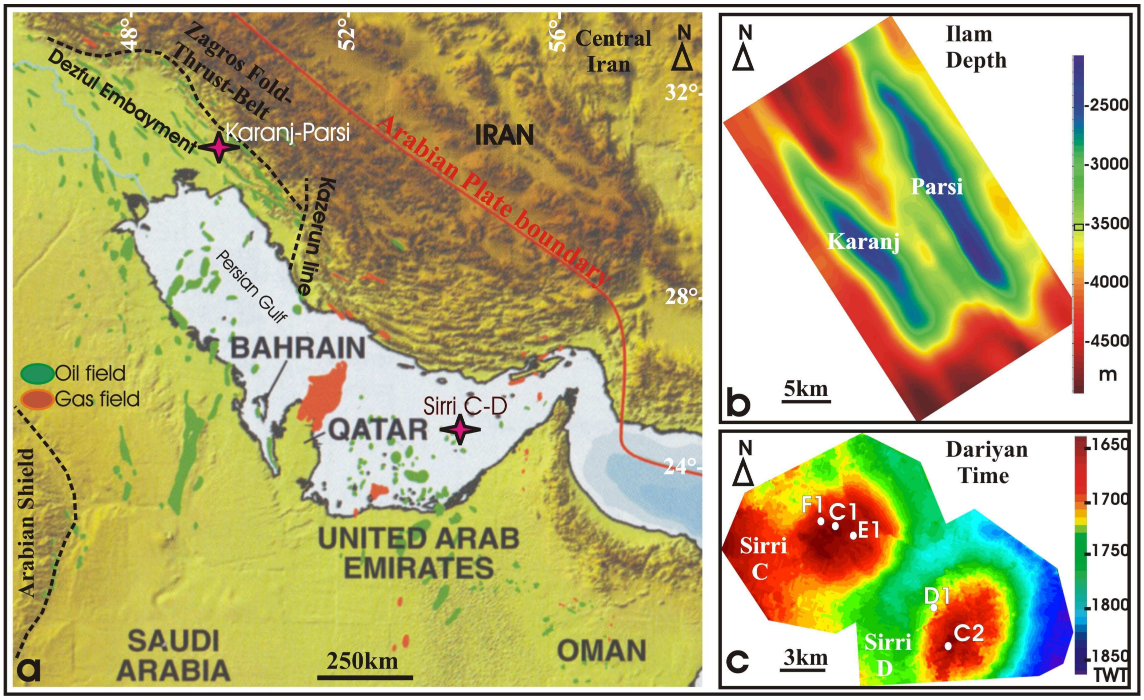
48°
52°
56°
Central Iran
N
32°
28°
24°
Zagros Fold-Thrust-Belt
Dezful Embayment
Karanj-Parsi
IRAN
Arabian Plate boundary
Kazerun line
Persian Gulf
BAHRAIN
Oil field
Gas field
QATAR
Sirri C-D
Arabian Shield
UNITED ARAB EMIRATES
SAUDI ARABIA
250km
OMAN
a
Ilam Depth
Parsi
Karanj
-2500
-3000
-3500
-4000
-4500
m
5km
b
Dariyan Time
F1
C1
E1
Sirri C
D1
C2
Sirri D
1650
1700
1750
1800
1850
TWT
3km
c

Figure 1

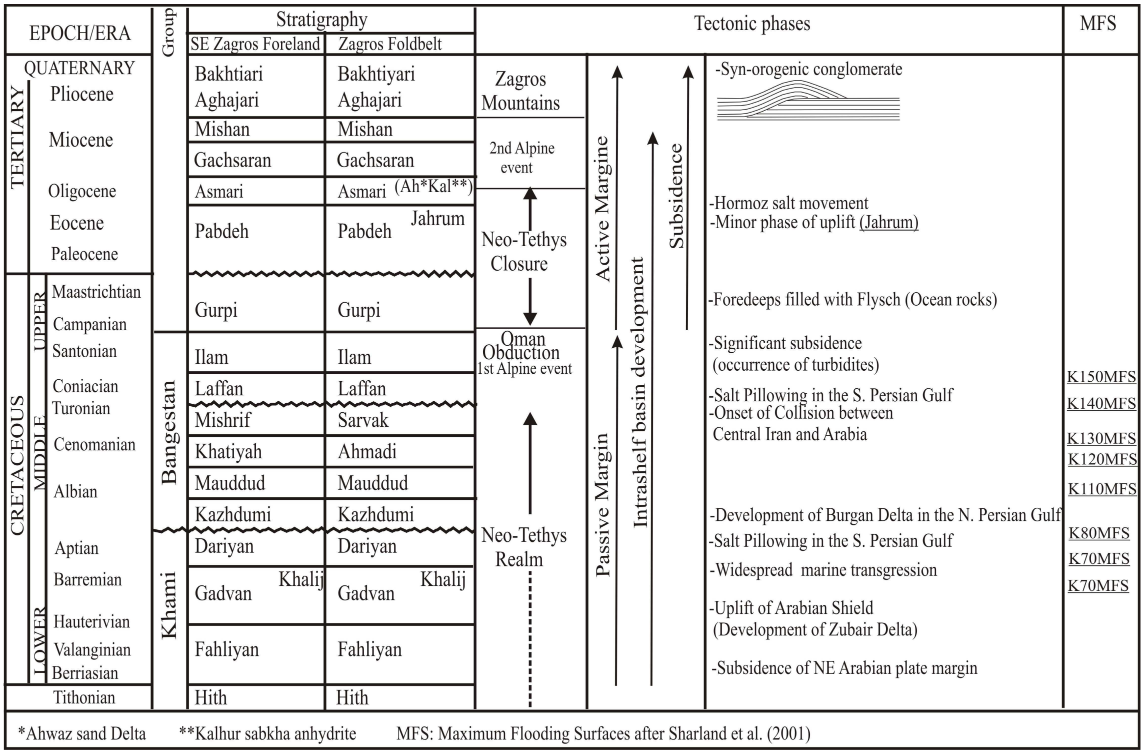
EPOCH/ERA
Group
Stratigraphy
SE Zagros Foreland
Zagros Foldbelt
Tectonic phases
MFS
QUATERNARY
TERTIARY
Pliocene
Miocene
Oligocene
Eocene
Paleocene
CRETACEOUS
UPPER
MIDDLE
LOWER
Maastrichtian
Campanian
Santonian
Coniacian
Turonian
Cenomanian
Albian
Aptian
Barremian
Hauterivian
Valanginian
Berriasian
Tithonian
Bangestan
Khami
Bakhtiari
Aghajari
Bakhtiyari
Aghajari
Mishan
Mishan
Gachsaran
Gachsaran
Asmari
Asmari (Ah*Kal**)
Pabdeh
Pabdeh
Jahrum
Gurpi
Gurpi
Ilam
Ilam
Laffan
Laffan
Mishrif
Sarvak
Khatiyah
Ahmadi
Mauddud
Mauddud
Kazhdumi
Kazhdumi
Dariyan
Dariyan
Gadvan
Khalij
Gadvan
Khalij
Fahliyan
Fahliyan
Hith
Hith
Zagros Mountains
2nd Alpine event
Neo-Tethys Closure
Oman Obduction
1st Alpine event
Neo-Tethys Realm
Active Margine
Passive Margin
Intrashelf basin development
Subsidence
-Syn-orogenic conglomerate
-Hormoz salt movement
-Minor phase of uplift (Jahrum)
-Foredeeps filled with Flysch (Ocean rocks)
-Significant subsidence (occurrence of turbidites)
-Salt Pillowing in the S. Persian Gulf
-Onset of Collision between Central Iran and Arabia
-Development of Burgan Delta in the N. Persian Gulf
-Salt Pillowing in the S. Persian Gulf
-Widespread marine transgression
-Uplift of Arabian Shield (Development of Zubair Delta)
-Subsidence of NE Arabian plate margin
K150MFS
K140MFS
K130MFS
K120MFS
K110MFS
K80MFS
K70MFS
K70MFS
*Ahwaz sand Delta
**Kalhur sabkha anhydrite
MFS: Maximum Flooding Surfaces after Sharland et al. (2001)

Figure 2

Table 1

EPOCH/ERA		Group	Stratigraphy SE Zagros Foreland	Interval velocity m/s	Stratigraphy Zagros Foldbelt	Remarks
QUATERNARY		Bangestan				
TERTIARY	Pliocene		Bakhtiari Aghajari	2200......................4000	Bakhtiyari Aghajari	
	Miocene		Mishan		Mishan	
			Gachsaran	4450	Gachsaran	-Ahwaz(Ah) sand-3500m/s Kalhur Anhydrite (Kal)-5000m/s Salt-4450
	Oligocene		Asmari	4000......................5750	Asmari (Ah*Kal**)	
	Eocene, Paleocene		Pabdeh	4000......................4750	Pabdeh Jahrum	
CRETACEOUS UPPER	Maastrichtian, Campanian		Gurpi		Gurpi	
	Santonian		Ilam		Ilam	-Interval velocities generally lower than sarvak
	Coniacian		Laffan		Laffan	
CRETACEOUS MIDDLE	Turonian		Mishrif	5500......................6000	Sarvak	-Uniform velocity variation with depth
	Cenomanian		Khatiyah			
	Albian		Mauddud			
			Kazhdumi	3500......................4000	Kazhdumi	-Kazhdumi/Sarvak boundary is an important regional velocity inversion
CRETACEOUS LOWER	Aptian	Khami	Dariyan	5000......................6000	Dariyan	-Negative velocity gradient in Kazhdumi can be attributed to over-pressure zones
	Barremian		Gadvan Khalij	4100......................6000 3750......................4300	Gadvan Khalij	-No strong regional velocity trend in Dariyan. Velocity is controlled by depositional/post-depositional factors -Khalij limestone does not show depth-dependent velocity variation
	Hauterivian, Valanginian, Berriasian		Fahliyan	?	Fahliyan	
Tithonian			Hith	?	Hith	

*Ahwaz sand Delta **Kalhur sabkha anhydrite

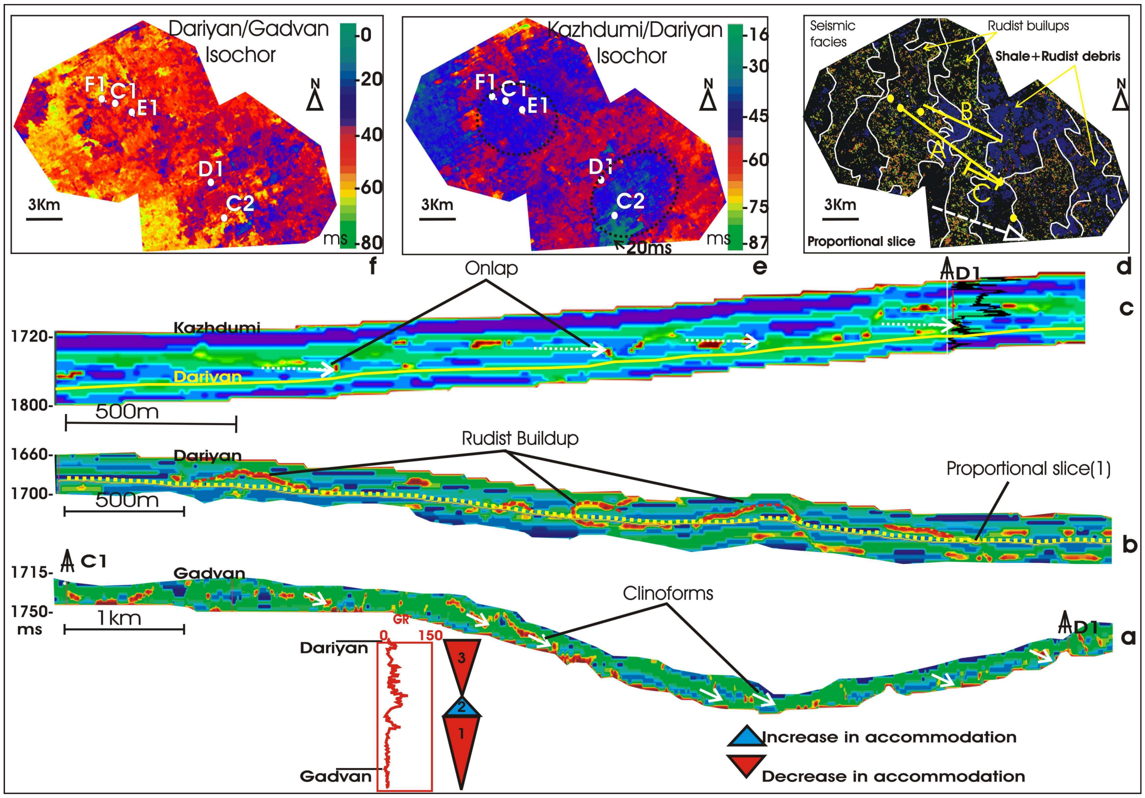

Dariyan/Gadvan Isochor
F1
C1
E1
D1
C2
3Km
ms
0
20
40
60
80
f
Kazhdumi/Dariyan Isochor
20ms
e
Seismic facies
Rudist builups
Shale+Rudist debris
Proportional slice
d
Onlap
D1
c
Kazhdumi
Dariyan
1720-
1800-
500m
Rudist Buildup
Proportional slice(1)
1660-
1700-
b
C1
Gadvan
1715-
1750-
ms
1km
Clinoforms
a
Dariyan
GR
0
150
Gadvan
3
2
1
Increase in accommodation
Decrease in accommodation

Figure 3

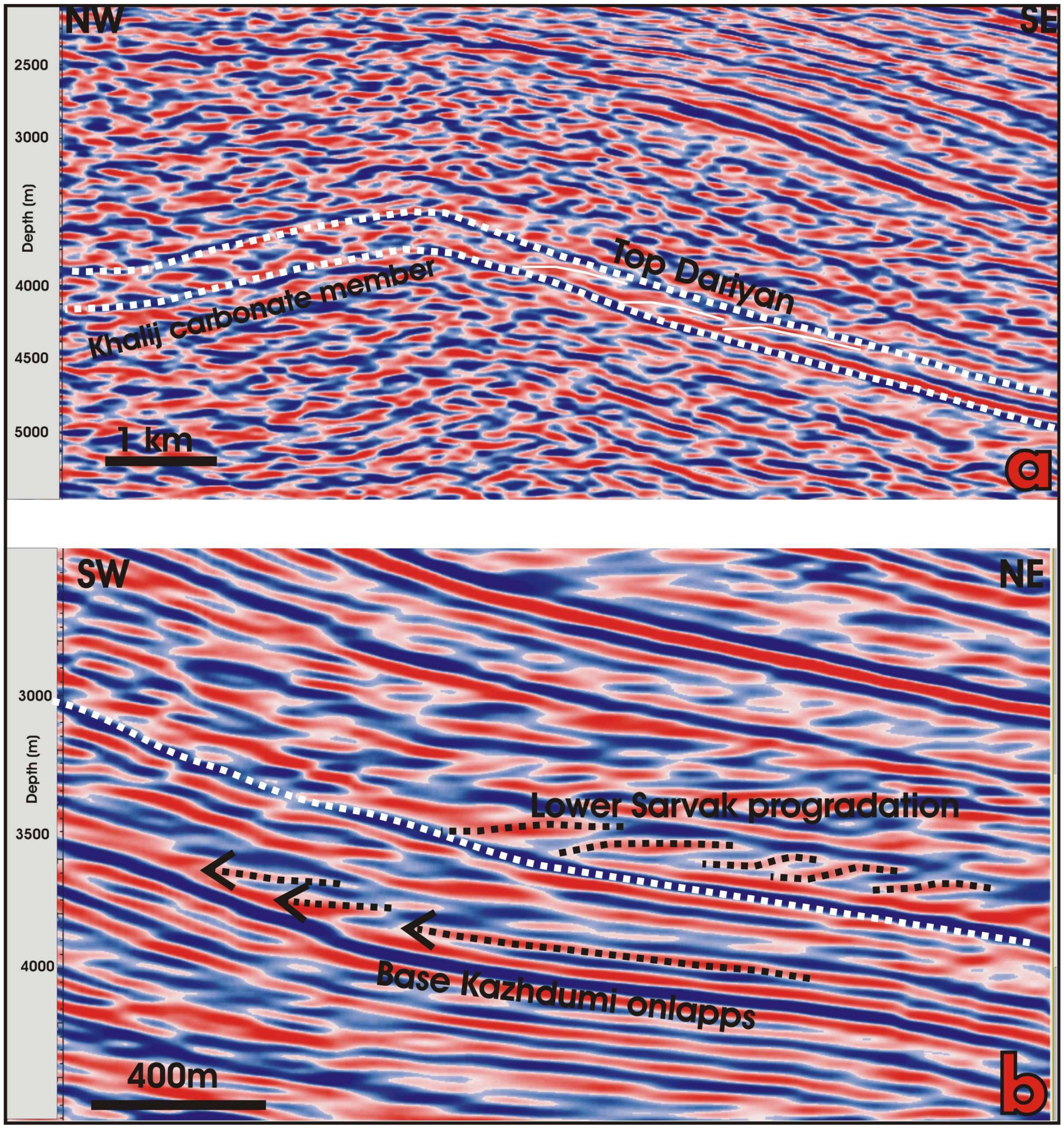
NW
SE
2500
3000
Depth (m)
4000
4500
5000
Top Dariyan
Khalij carbonate member
1 km
a
SW
NE
3000
Depth (m)
3500
4000
Lower Sarvak progradation
Base Kazhdumi onlapps
400m
b

Figure 4

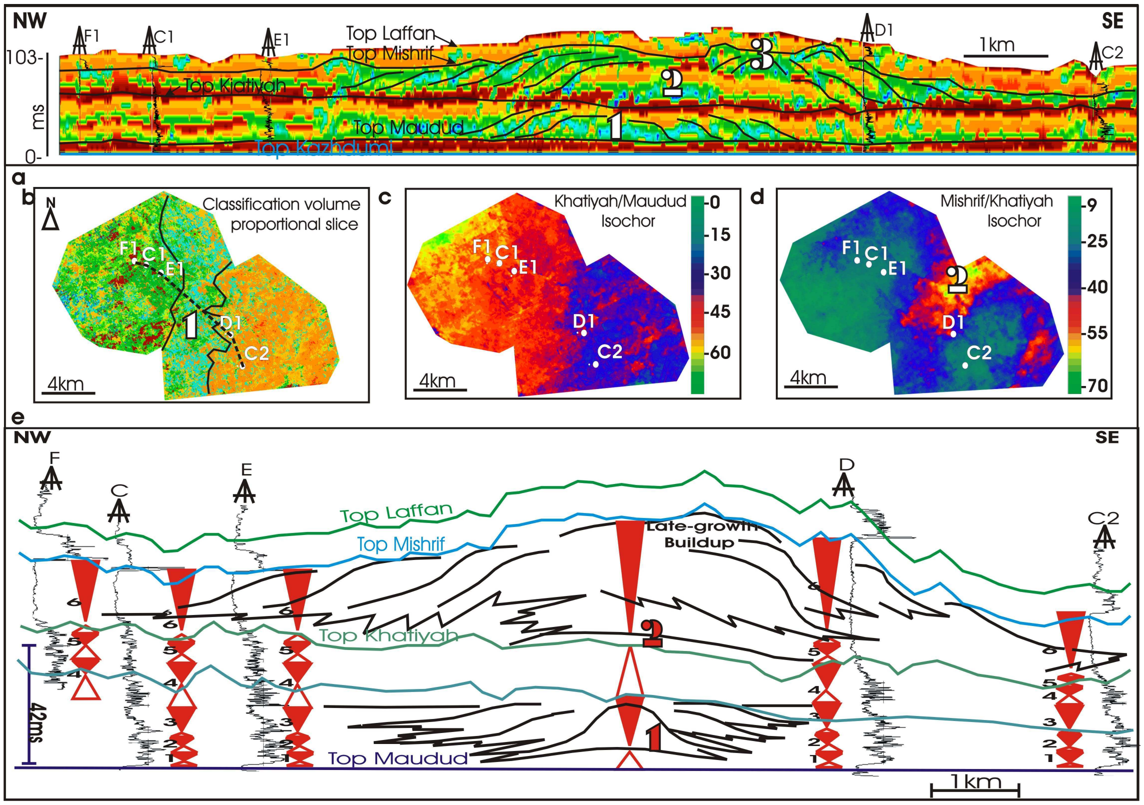
NW
SE
F1
C1
E1
D1
C2
Top Laffan
Top Mishrif
Top Khatiyah
Top Maudud
Top Kazhdumi
1km
103-
0-
ms
1
2
3
a
b
N
Classification volume proportional slice
4km
c
Khatiyah/Maudud Isochor
-0
-15
-30
-45
-60
d
Mishrif/Khatiyah Isochor
-9
-25
-40
-55
-70
e
F
C
E
D
Late-growth Buildup
42ms
1km

Figure 5

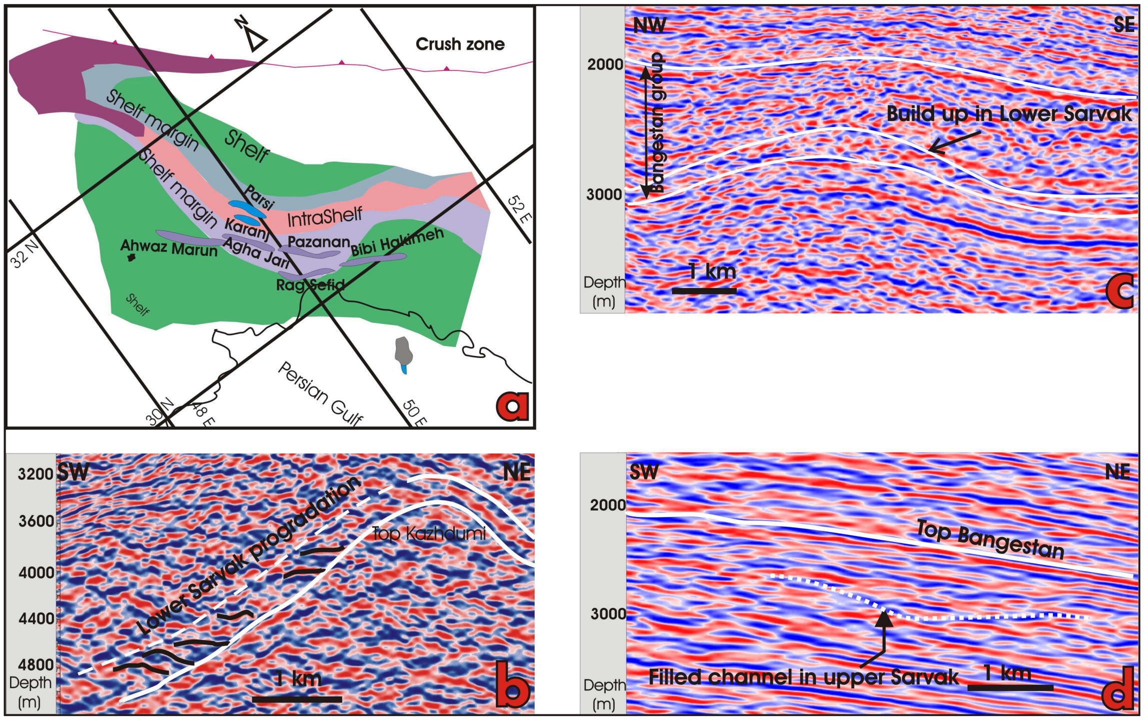
Crush zone
N
Shelf margin
Shelf
Shelf margin
Parsi
IntraShelf
Karanj
Pazanan
Bibi Hakimeh
Ahwaz Marun
Agha Jari
Rag Sefid
Shelf
Persian Gulf
32 N
30 N
48 E
50 E
52 E
a
NW
SE
2000
3000
Bangestan group
Build up in Lower Sarvak
Depth (m)
1 km
c
SW
NE
3200
3600
4000
4400
4800
Depth (m)
Lower Sarvak progradation
Top Kazhdumi
1 km
b
SW
NE
2000
3000
Top Bangestan
Filled channel in upper Sarvak
1 km
Depth (m)
d

Figure 6

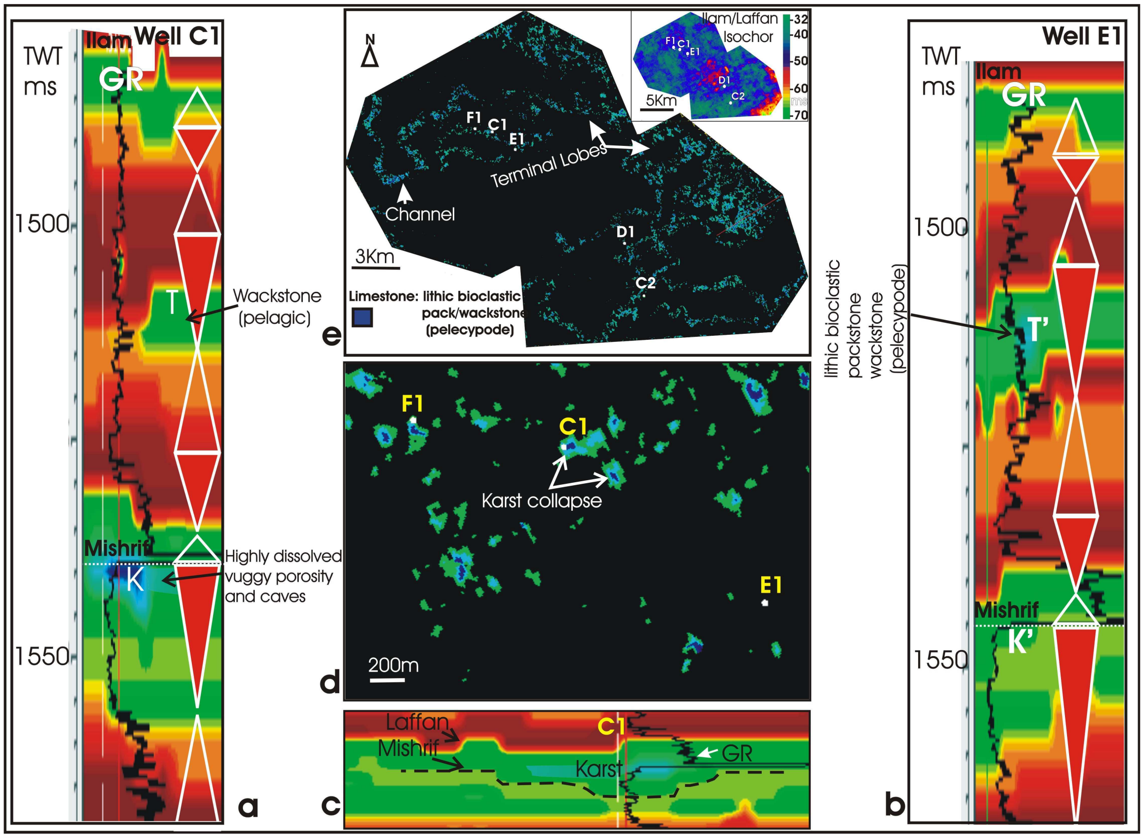

Well C1
TWT
ms
Ilam
GR
1500
Wackstone
(pelagic)
T
Mishrif
K
Highly dissolved
vuggy porosity
and caves
1550
a
N
F1
C1
E1
Terminal Lobes
Channel
D1
C2
3Km
Ilam/Laffan
Isochor
5Km
-32
-40
-50
-60
-70
Limestone: lithic bioclastic
pack/wackstone
(pelecypode)
e
Karst collapse
200m
d
Laffan
Mishrif
Karst
GR
c
Well E1
TWT
ms
Ilam
GR
1500
lithic bioclastic
packstone
wackstone
(pelecypode)
T'
Mishrif
K'
1550
b

Figure 7

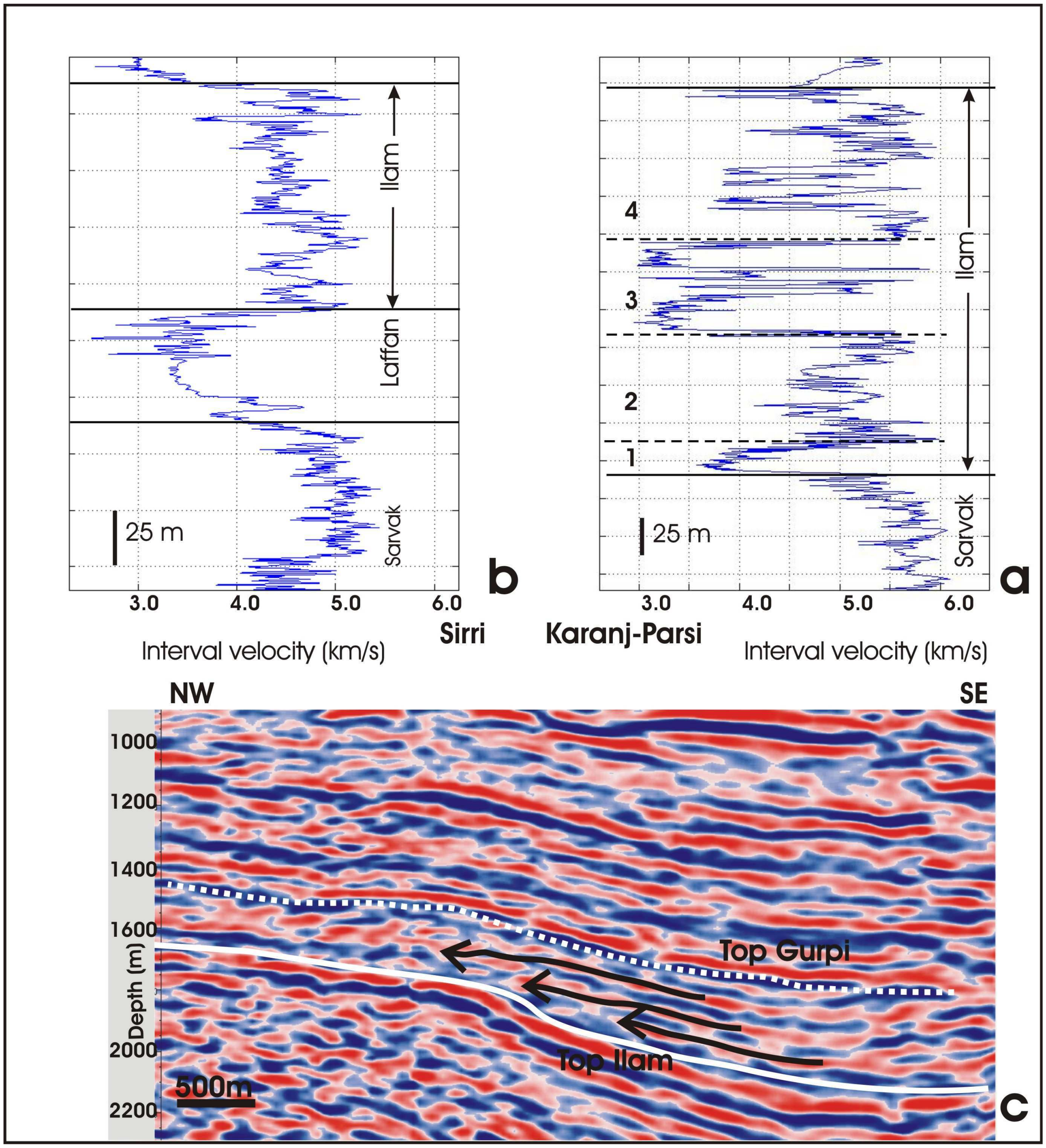
Ilam
Laffan
Sarvak
25 m
b
3.0
4.0
5.0
6.0
Interval velocity (km/s)
Sirri
Karanj-Parsi
4
3
2
1
Ilam
Sarvak
25 m
a
Interval velocity (km/s)
NW
SE
1000
1200
1400
1600
Depth (m)
2000
2200
Top Gurpi
Top Ilam
500m
c

Figure 8

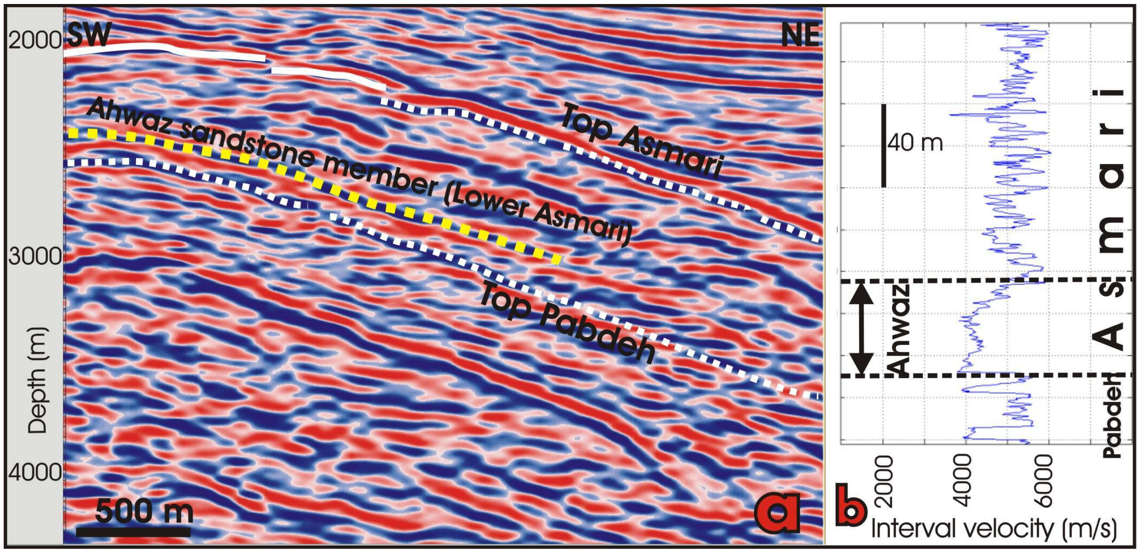

2000
3000
4000
Depth (m)
SW
NE
Top Asmari
Ahwaz sandstone member (Lower Asmari)
Top Pabdeh
500 m
a
b
40 m
Ahwaz
Asmari
Pabdeh
2000
4000
6000
Interval velocity (m/s)

Figure 9

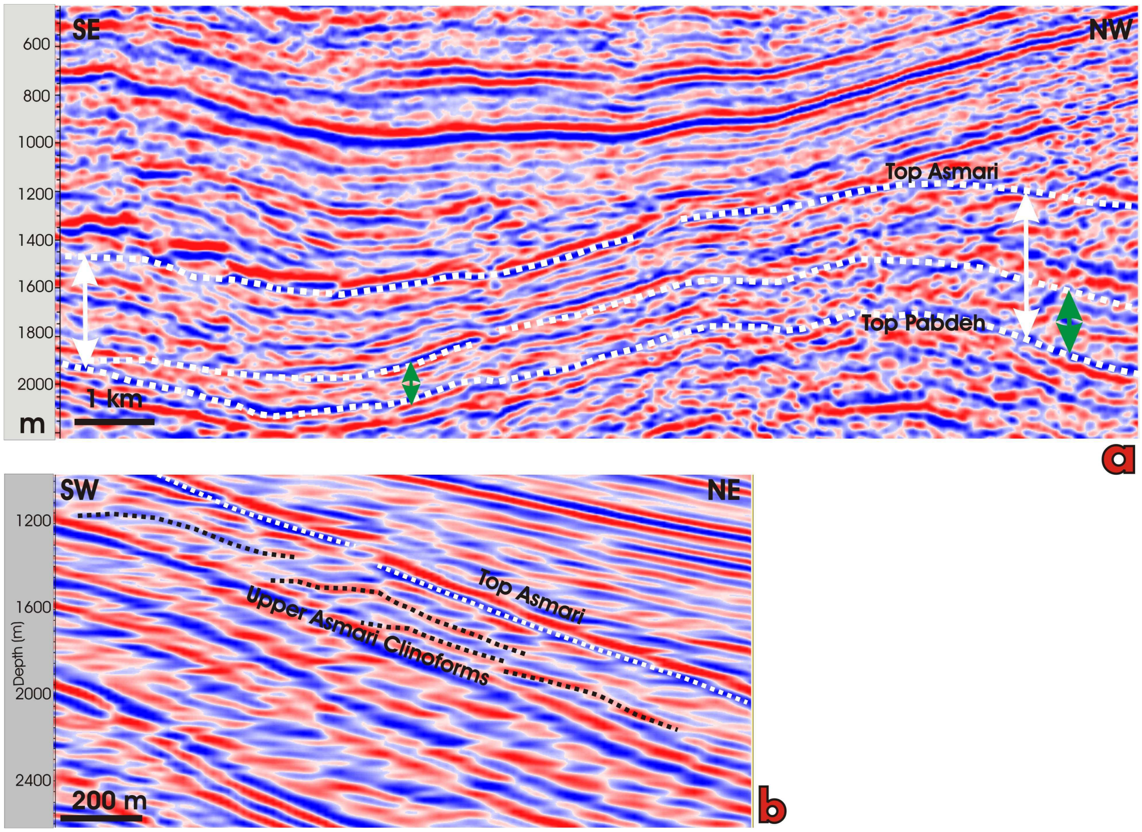
SE
NW
600
800
1000
1200
1400
1600
1800
2000
m
1 km
Top Asmari
Top Pabdeh
a
SW
NE
1200
1600
2000
2400
Depth (m)
Top Asmari
Upper Asmari Clinoforms
200 m
b

Figure 10

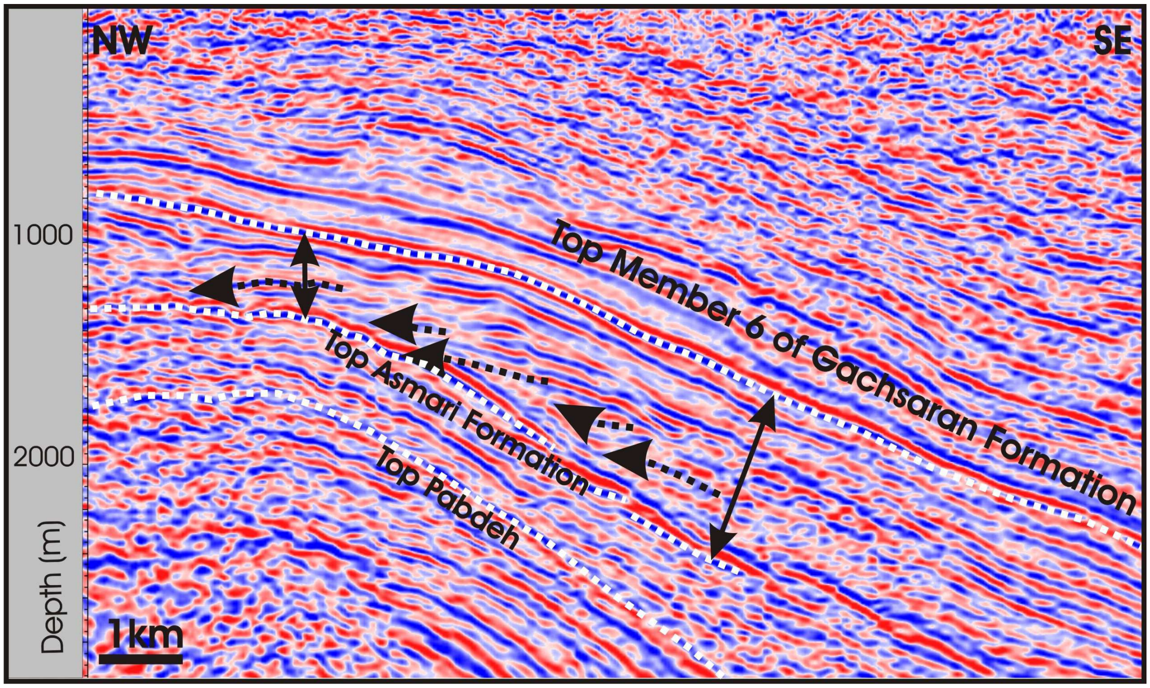
NW
SE
1000
2000
Depth (m)
1km
Top Member 6 of Gachsaran Formation
Top Asmari Formation
Top Pabdeh

Figure 11